View metadata, citation and similar papers at core.ac.uk

brought to you by CORE

provided by The University of Utah: J. Willard Marriott Digital Library

USING GROUNDWATER TRANSIT TIMES DETERMINED FROM ENVIRONMENTAL TRACER CONCENTRATIONS TO ASSESS STORAGE WITHIN A WATERSHED

by

Jennifer Lynn Georgek

A thesis submitted to the faculty of
The University of Utah
in partial fulfillment of the requirements for the degree of

Master of Science

in

Geology

Department of Geology and Geophysics

The University of Utah

May 2016

Copyright © Jennifer Lynn Georgek 2016

All Rights Reserved

The University of Utah Graduate School

STATEMENT OF THESIS APPROVAL

The thesis of **Jennifer Lynn Georgek**

has been approved by the following supervisory committee members:

Douglas Kip Solomon	, Chair	**3/10/16** Date Approved
Victor Michael Heilweil	, Member	**3/10/16** Date Approved
Paul Jewell	, Member	**3/14/16** Date Approved

and by **John M. Bartley** , Chair/Dean of

the Department/College/School of **Geology and Geophysics**

and by David B. Kieda, Dean of The Graduate School.

ABSTRACT

Previous watershed assessments have relied on annual baseflow estimates to provide an improved, albeit limited, understanding of the groundwater contribution to surface water bodies. In order to quantify the volume of groundwater in storage, additional information such as groundwater mean transit time (MTT) is needed. In this study, several approaches were evaluated for determining the groundwater MTT in the West Fork Duchesne River watershed in northeastern Utah. The most promising result was obtained with lumped-parameter modeling (LPM) of environmental tracers (SF_6, CFCs, and $^3H/^3He$) from 21 springs within the catchment. Approximately 30% of the springs exhibited an exponential transit time distribution (TTD); the remaining ~ 70% were best characterized by a piston-flow TTD. The flow-weighted groundwater MTT for the West Fork watershed is about 40 years with approximately 20 years spent in the unsaturated zone. A cumulative distribution of these ages revealed that a majority of the groundwater within the catchment is between 30 and 50 years old. As a result, the West Fork is considered a fairly stable catchment; it is hypothesized that short-term changes in recharge brought about by 5-10 year droughts are unlikely to have as profound effect on this watershed as compared to systems with shorter MTTs. A chemical hydrograph separation of West Fork stream flow estimated the average annual baseflow to be ~ 1.7 x 10^7 m^3/year, which was assumed to be a proxy for groundwater discharge from the watershed. Using

this MTT and baseflow estimation, the volume of mobile groundwater stored in the West Fork watershed was calculated to be ~ 6.5×10^8 m^3. This volume translates to an average saturated zone thickness of ~ 20 m, or a recharge rate of ~ 0.09 m/year over the area of the watershed. In addition to spring sampling, several nonvolatile tracers (major ions, dissolved silica, and tritium) were evaluated in stream water. Over the scale of the watershed studied, there was no apparent correlation between major ions, or silica, and groundwater age. Furthermore, the usefulness of baseflow tritium (^3H) was significantly limited given the fact that atmospheric ^3H records in the region have only recently stabilized. Future watershed-scale assessments should evaluate groundwater MTT, in addition to annual baseflow, in order to quantify groundwater storage and more accurately assess watershed susceptibility to development and climate variability.

TABLE OF CONTENTS

LIST OF TABLES

LIST OF FIGURES

ACKNOWLEDGEMENTS

Completion of this project would not have been possible without the support and expertise of my advisor, Dr. Kip Solomon and committee members, Vic Heilweil and Paul Jewell. Thank you.

I am also indebted to numerous employees at the United States Geological Survey (USGS) Utah Water Science Center who provided funding, and aided in fieldwork, planning, and project development - especially David Susong, Matt Miller, John Solder, John Carricabaru, Christine Rumsey, Tom Marston, and Chris Shope.

And to my peers, and superiors, at the University of Utah - thank you for your patience, guidance, and most of all, your friendship. It's been a pleasure working with you, Wil Mace, Alan Rigby, Cedar Coleman, Stewart Gubler, Olivia Miller, and Nora Nelson.

And finally, thank you to my parents and brothers whose immeasurable amount of love and support has given me the determination to pursue my dreams in lieu of all of life's obstacles.

1 INTRODUCTION

1.1 Groundwater Mean Transit Time

Groundwater can be a significant fraction of stream discharge, especially in arid to semiarid regions like the western U.S. where runoff depends predominantly on wintertime precipitation. Miller et al. (2014) determined the average annual baseflow for 14 streams and rivers in the Upper Colorado River Basin to be 21-58% of stream discharge. During periods of low-flow (not including spring snowmelt), this percentage of baseflow as part of total stream flow was as great as 86% (Miller et al., 2014). Similar results were reported by Frisbee et al. (2011) for the Saguache Creek watershed in the San Juan Mountains, in which the maximum groundwater component was 78% of stream discharge during baseflow conditions. These results stress the importance of understanding the groundwater within a watershed, but baseflow alone does not provide any information about the volume of groundwater in storage.

Groundwater mean transit time (MTT), or the amount of time water travels through the subsurface from a recharge location to a discharge location, is defined as follows (Cook and Böhlke, 2000):

$$\tau = \frac{V}{Q} \tag{1}$$

where, τ is MTT, V is the volume of groundwater in storage, and Q is the rate at which the water is discharging. Assuming that baseflow is representative of groundwater discharge (Q), we postulate that baseflow estimates can be used in conjunction with groundwater age determinations to calculate the volume of groundwater stored within a watershed, and assess groundwater susceptibility to water withdrawals, changes in climate, and (or) changes in land use that could affect recharge rates in a given region.

1.2 Groundwater Dating

Groundwater age has commonly been determined using environmental tracer concentrations in groundwater (e.g., Busenberg and Plummer, 1992; Cook and Solomon, 1997; Koh et al., 2007). Atmospheric concentrations of sulfur hexafluoride (SF_6) and chlorofluorocarbons (CFCs) have been well-recorded throughout the past 60 years. Because these tracers are present in infiltration, their air-equivalent concentrations can be used for groundwater dating. Similarly, thermonuclear testing from 1952 to 1963 created a spike in atmospheric tritium concentrations that resulted in another useful method for evaluating groundwater age based on ratios of tritium (^3H) to helium-3 (^3He) - the radioactive decay product of ^3H (Solomon and Cook, 2000). This study utilizes all of these tracers in order to evaluate the groundwater age distribution within the West Fork watershed.

However, because some of these tracers are volatile, their usefulness for dating groundwater depends on the accuracy to which infiltration, and subsurface transit, is characterized in order to account for gas exchange with the atmosphere. For example, CFC and SF_6 ages are sensitive to recharge temperature, recharge elevation (e.g., barometric pressure), excess air, and a number of other factors including the potential for contamination, microbial degradation, and sorption (Solomon and Cook, 2000). These factors not only necessitate careful sampling, but also require a number of correction factors, each of which contributes additional uncertainty to age results.

1.2.1 Nonvolatile Tracers

Use of a nonvolatile dissolved constituent for determining groundwater mean transit time within a watershed would allow data collection to be done in-stream. As a result, future large-scale watershed assessments could be more comprehensive with only a minimal expenditure of time and resources. Peters et al. (2014) compared dissolved silica content to $^{3}H/^{3}He$ ages in groundwater within the Panola Mountain Research Watershed (PMRW) in Georgia - a small (0.41 km^2) catchment dominated by granitic bedrock. Greater concentrations of dissolved silica generally correlated to older groundwater ages, a result attributed to the more prolonged interaction of this water with the subsurface environment, i.e., longer MTTs (Peters et al., 2014). Morgenstern et al. (2010) reported similar results for the Toenapi catchment in New Zealand, in which the lowest ^{3}H concentrations - representative of the oldest waters - correlated to higher dissolved silica (SiO_2) concentrations. In the West Fork watershed, groundwater silica concentrations were compared to groundwater ages from springs within the watershed in order to assess the applicability of this silica-age relationship to yet another hydrogeologic setting. A variety of major anions and cations were also assessed for a potential correlation between concentrations and groundwater age.

Another nonvolatile method, relying solely on groundwater ^{3}H concentrations, was investigated in the West Fork watershed. Measurement of ^3H in groundwater, in combination with ^3He, is a well-established method for determining groundwater transit times (e.g., Schlosser et al., 1988; Solomon et al., 1993; Kralik et al., 2014). For many locations, enough time has passed since initial bomb-testing to allow for sufficient decay of this ^3H, and the stabilization of atmospheric ^3H back to natural cosmogenic levels (Eastoe et al., 2012). This is especially the case in the Southern Hemisphere which received only about 5% of the nuclear-test ^3H released into the atmosphere (Morgenstern et al., 2010). As a result, this thermonuclear-sourced ^3H has not been detectable for nearly 20 years at southern latitudes. This has allowed for the assessment of groundwater transit times for several watersheds in New Zealand based on ^3H concentrations (Stewart et al., 2007; Morgenstern et al., 2010). Even for a variety of locations in the southwestern United States, average ^3H levels in precipitation have been relatively constant since ~2005 (Morgenstern et al., 2010). This recent stabilization in atmospheric ^3H levels may provide an unambiguous age-dating method for relatively young (<10 year old) groundwater.

2 STUDY SETTING

2.1 Geography and Climate

The West Fork Duchesne River watershed was selected for this study as a result of elevated ^{222}Rn measured in West Fork stream water by the United States Geological Survey (USGS) Utah Water Science Center in November 2013 (Chris Shope, written communication, November 2013); higher in-stream concentrations of ^{222}Rn can be indicative of groundwater inflow (Genereux and Hemond, 1990; Cook et. al., 2003). This headwater catchment (~ 181 km^2) is located in northeastern Utah within the northern Uinta Basin of the larger Upper Colorado River Basin (UCRB) (Figure 1) (Utah AGRC, 2016). Stream flow is from west to east, and extends nearly 29 km before joining the North Fork and the main channel of the Duchesne River. West Fork elevations range from nearly 2,900 m above sea level (MASL) at the uppermost headwaters to approximately 2,100 MASL at the North Fork confluence. The main channel is meandering and varies from ~3 to ~12 m in width. A substantial number of beaver dams have been constructed throughout the downstream extent of the West Fork and are responsible for diverting flow into multiple channels where the valley widens. Mean annual air temperature within the watershed is between ~ 4 to 6 °C (PRISM Climate Group, 2015), and annual precipitation varies from ~ 0.38 - 0.64 m/year at lower elevations, to ~ 0.64 -0.89 m/year in the upper, headwater locations (PRISM Climate Group, 2014).

Figure 1. Shaded relief map of the West Fork watershed (Utah AGRC, 2016). The watershed is highlighted in blue. A total of twenty-one spring sampling locations are denoted by the red circles. Springs *A-D* lie along a headwater tributary called the Little West Fork. Letters on the map correspond to the following sampling location names: A = *LWFDS01*, B = *LWFDS05*, C = *New Spring #4*, D = *LWFDS07*, E = *WFDS09*, F = *WFDS08*, G = *WFDS10*, H = *WFDS12*, I = *West Fork (W.F.) Upper Spring*, J = *Upper Spring B*, K = *New Spring #1*, L = *New Spring #2*, M = *New Spring #3*, N = *West Fork (W.F.) Lower Spring*, O = *WFDS13*, P = *WFDS14*, Q = *Five Suns Spring*, R = *South (S.) Side Spring #1*, S = *WFDS19*, T = *FR050 Spring*, U = *North (N.) Side Spring #1*. The star denotes the approximate location of the West Fork Gage site, and the "X" gives the approximate location of the stream sampling site above the Vat Dam.

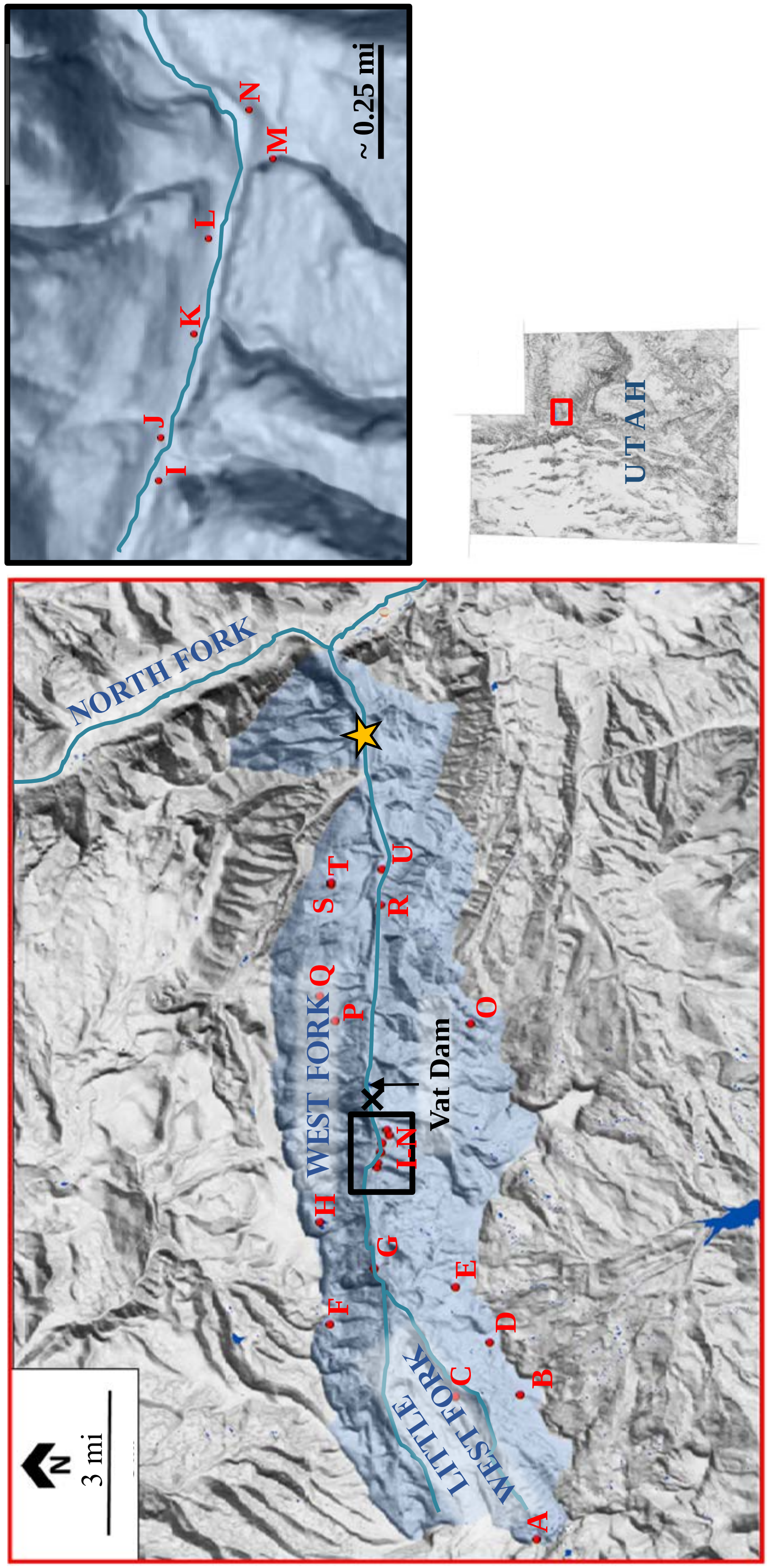
~ 0.25 mi
I
J
K
L
M
N
UTAH
NORTH FORK
WEST FORK
LITTLE WEST FORK
Vat Dam
3 mi
N
A
B
C
D
E
F
G
H
L-N
O
P
Q
R
S
T
U

The Vat Dam, located mid-reach along the West Fork, diverts a substantial amount of West Fork stream flow each year (Figure 1) (CUWCD, 2015). Daily diversion records were provided by the Central Utah Water Conservancy District (CUWCD) in Duchesne, Utah for March 2014 to March 2015 (Appendix A). These data were used in the chemical hydrograph separation analysis for estimating annual baseflow upstream of the dam. Diversions typically begin at the end of April with approximately 0.14 - 0.57 m^3/s (5 to 20 cfs), and then gradually increase to a maximum of about 4.25 m^3/s in mid- to late-May. Diversions decrease throughout the beginning of June, and remain relatively low, or at 0 m^3/s, for the remaining months of the year. At the Vat Dam, discharge typically ranges between 0.14 - 0.28 m^3/s (5-10 cfs) during baseflow conditions, to upwards of 560 m^3/s (~200 cfs) during late spring and early summer.

2.2 Geology

Higher elevations within the West Fork watershed are dominated by the coarse clastic units of the Uinta Formation (~ 150 - 275 m thick). This unit is comprised of conglomerates interbedded with mudstone, and to a lesser degree, coarse-grained sandstones; cement containing bentonite clay is present primarily to the southeast of the West Fork watershed (Constenius et al., 2011).

In the upper half of the catchment, the north slope of the watershed exposes several other principal lithologic units, including: the upper Eocene Keetley Volcanics, the lower members of the Middle Jurassic Twin Creek Limestone, the Nugget (Navajo) Sandstone, and the mudstones and sandstones of the Upper and Lower Triassic Ankareh Formation (Figure 2). Unit thicknesses in this region are approximately 0 – 430 m, or more, for the

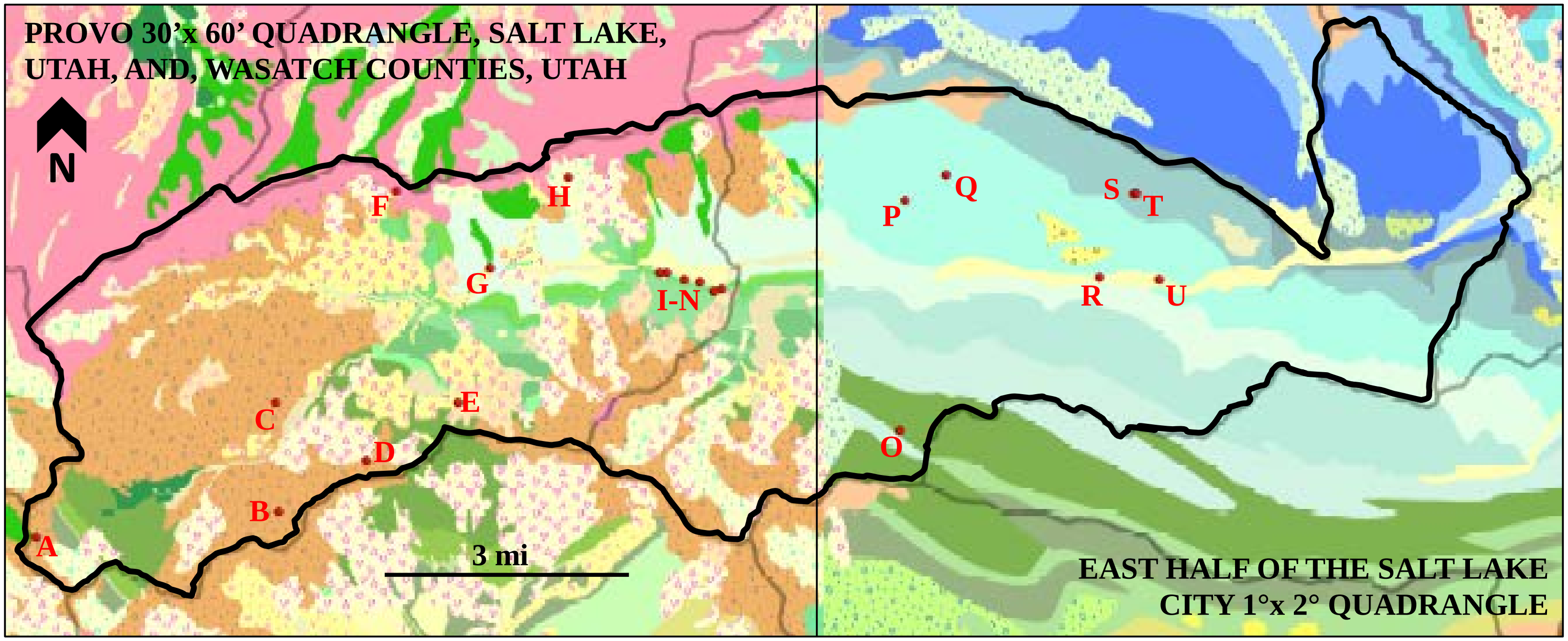

Relevant Map Units

Qa	Alluvium	Kcm	Cedar Mountain Formation	T_Ra	Ankareh Formation
Qmc	Mass-movement and colluvial deposts	Jp	Preuss Formation	T_Rt	Thaynes Limestone
Qmg	Mass-movement and glacial deposits	Jtrsg	Twin Creek Limestone	Pp	Park City Formation
Tk	Keetley Volcanics	Jtw	Twin Creek Limestone	PPw	Weber Sandstone
Tucb	Uinta Formation	Jn	Nugget Sandstone		

Figure 2. Geologic map of the West Fork watershed (outlined in black) (Utah AGRC, 2010; Constenius et al., 2011; Bryant, 2010). Spring sampling locations are denoted by red circles. Letter references to site names can be found in Figure 1.

Keetley Volcanics, ~240 m for the Twin Creek, ~400 m for the Nugget, and ~500 m for the Ankareh. In general, beds dip between 20 - 30 degrees to the S-SW; as a result, several (younger) units are present in outcrop on the south slope of the watershed that are not present on the north slope. These include the upper members of the Twin Creek Limestone, as well as the Middle Jurassic sandstones of the Preuss Formation (~230 m thick in this region) (Constenius et al., 2011).

The lower half of the catchment reveals several older bedrock units. Lower Permian to Middle Pennsylvanian Weber Sandstone (~300-500 m thick), the Permian Park City Formation that is comprised of limestone, siltstone, sandstone, and phosphatic shale (~100 m thick), and the Lower Ankareh Formation dominate lower elevation north-slope geology (Bryant, 2010). The Nugget Sandstone, Twin Creek Limestone, and the sandstones of the Cedar Mountain Formation (~355 - 810 m thick) are exposed on the corresponding south slope (Bryant, 2010).

2.3 Hydrogeology

In general, the geologic units in the West Fork watershed are fairly permeable. Gee (1994) reported groundwater inflow rates of more than 545 m^3/day (100 gal/min) in mines and tunnels in Park City, Utah, that penetrate the Thaynes Limestone, the Park City Formation, and the Weber Sandstone. Freeze and Cherry (1979) provide porosity ranges of 0.00 – 0.20 for limestone and 0.05 – 0.30 for sandstone. More specifically, for the Nugget Sandstone – one of the primary units in the upper reaches of the West Fork - mean total porosity (η) has been determined to average ~0.19 in Utah and southwestern Wyoming, with values as high as 0.35 in some locations (Uygur and Picard, 1984).

Additionally, Freethey and Cordy (1991) analyzed over 100 laboratory samples of the Nugget and concluded that nearly 60% of the samples had hydraulic conductivities (*K*) of 0.03 -0.3 m/day (0.1 - 1 ft/day), with nearly 26% having *K* values between 0.3 - 3 m/day (1 - 10 ft/day). The estimated transmissivity (*T*) of the Nugget aquifer (~465 m^2/day or ~5,000 ft^2/day) is also fairly high as a result of its considerable thickness (Freethey and Cordy, 1991). Freethey and Cordy (1991) estimated that the storage coefficient (*S*) of the (confined) Nugget aquifer ranges from 0.0003 – 0.008, and the estimated specific yield (S_y) is ~0.05 – 0.10 (unconfined aquifer percent).

Despite the dominance of highly permeable sandstone and limestone within the watershed, there are several confining layers within these geologic units. These include shales in the Preuss Formation, shales and siltstones in the Gypsum Spring Member and Boundary Ridge Members of the Twin Creek Limestone, mudstones in the Mahogany Member and upper member of the Ankareh Formation, as well as phosphatic shales in the Park City Formation (Ashland et al., 2001).

The presence of these confining units, and the overall geologic heterogeneity within the West Fork, provide the possibility for a wide range of hydrologic characteristics which control the apparent groundwater age distribution within the watershed. For example, unconfined regions – those dominated by the Thaynes, Nugget, and Twin Creek Formations – are likely characterized by more uniform recharge to the water table. Groundwater discharge from these units could be a mix of both young and old water that has recharged from both near and far. Contrary to this unconfined conceptual model is a more heterogeneous model in which confining layers result in significant spatial variability for the rate at which recharge, and discharge, occurs throughout the catchment. In this case, recharge is considerably more localized, and as a result, discharging water likely reveals a more narrow age distribution. Both of these conceptual models are considered in this study.

3 METHODS

3.1 Sample Collection

3.1.1 Stream Sampling

Continuous and discrete stream sampling were necessary for the chemical hydrograph separation to estimate West Fork baseflow, and for the evaluation of nonvolatile dating methods. In March 2014, a multiparameter sonde (YSI 600R) was installed along the lower reaches of the West Fork Duchesne River in order to provide a continuous record of temperature, specific conductance (SC), and stream stage (via a pressure transducer) (Figure 1). Continuous stream data are provided in Appendix A. In addition to these continuous data, SF_6 , CFCs, and general chemistry samples were collected every 6-8 weeks at this gage site, and at a location just upstream of the Vat diversion (Figure 1).

General chemistry samples were collected for major cation and anion concentrations including: lithium (Li^+), ammonium (NH_4^+), calcium (Ca_2^+), magnesium (Mg^+), sodium (Na^+), potassium (K^+), bicarbonate (HCO_3^-), nitrite (NO_2^-), bromide (Br^-), nitrate (NO_3^-), phosphate (PO_4^{3-}), sulfate (SO_4^{2-}), chloride (Cl^-), and fluoride (F^-), as well as dissolved silica (SiO_2). During each sampling visit, temperature and SC were also measured using a Hydrolab Multiprobe. Stream SF_6 samples were collected in 1-liter amber glass bottles with polyseal cone-lined caps, and CFCs were collected in 125-mL glass bottles with aluminum lined caps. For stream sampling, SF_6 and CFCs were collected as grab samples in which the bottles were rinsed three times before being completely filled and then sealed underwater. Two SF_6 samples and at least three CFC samples were collected during each site visit. Stream chemistry samples were collected in 250 mL polyethylene bottles in the same manner as SF_6 and CFCs; however, capping underwater was not necessary. Stream SF_6 , CFC, and chemistry data are provided in Appendix A. Several stream ^3H samples were also collected (as grab samples) primarily during baseflow conditions in October 2014, and in January and February of 2015 (Table 3; Appendix A). Once collected, samples were stored in coolers and transported to the University of Utah for analysis.

3.1.2 Spring (Groundwater) Sampling

USGS topographic quadrangles, and field reconnaissance of the West Fork watershed, led to the identification and sampling of 21 springs for this study (Figure 1). These were located both near-channel, and at higher elevations off-channel, and were assumed to provide an accurate representation of the groundwater age distribution within the watershed.

Off-channel or high-elevation springs are defined in this study as springs located outside of the main channel of the West Fork at, or above, an elevation of 2,541 m – the median elevation of all springs sampled. The dataset includes 9 high-elevation springs which were mainly sampled in July 2014. The remaining 12 springs are categorized as near-channel given their proximity to the West Fork Duchesne River. Most near-channel springs were sampled during baseflow conditions in November 2013, or October 2014.

Temperature, SC, pH, dissolved oxygen (DO), barometric pressure, and total dissolved gas pressure (TDG) were measured at each spring using a Hydrolab Multiprobe. Field parameters for West Fork springs are provided in Appendix A.

SF_6 and CFC samples were collected following United States Geological Survey (USGS) sampling procedures provided on the USGS Reston Groundwater Dating Laboratory website (USGS, 2015). Spring samples for major cation and anion concentrations (including dissolved silica) were collected in the same manner as the stream samples described in Section 3.1.1. Chemistry samples were either filtered in-field using a 0.45-µm polypropylene membrane filter and then acidified with 2-mL of nitric acid for preservation, or were transported to the lab within several days of collection and filtered prior to analysis. Tritium samples were collected as grab samples, and noble gases were sampled with diffusion samplers, or inline copper tubes, according to the methods described on the University of Utah's Dissolved and Noble Gas Lab website (The University of Utah, 2015). Diffusion samplers were collected 1-7 days after initial deployment.

Discharge measurements were also made at a majority of the springs. Where necessary, earthen dams were constructed in order to divert spring discharge into a single channel. At most sites, a 3 in. Parshall flume was used to measure the depth of the diverted water which was later converted to discharge using the tables provided by the flume manufacturer. Several sampling locations were not suitable for the Parshall flume owing to inability to properly level the flume at the site. Instead, a stopwatch was used to determine the amount of time required for discharging water to fill a 3.5 gal bucket. Repeat measurements were made 3-5 times at each of these sites and the average of these trials was taken to be the spring discharge. At the largest spring in the dataset – Five Suns Spring - discharge was measured using a SonTek FlowTracker Handheld Flow Meter. Discharge measurements were not made at 3 of the 21 springs due to multiple discharge locations making a totalized measurement impractical, and/or other site characteristics which resulted in the inability to level the Parshall flume, or fill the 3.5 gal bucket.

3.2 Laboratory Analysis

SF_6 and CFCs were stripped from water samples and measured using a purge-and-trap gas chromatograph with electron capture detection (ECD) method in the University of Utah Environmental Tracers Laboratory. Tritium samples were first degassed in stainless steel flasks under high-vacuum using the extraction line in the University's Dissolved and Noble Gas Lab. Extracted samples were sealed and stored for approximately 3 months to allow for sufficient in-growth of ^{3}He which was then measured using a Helix magnetic sector-field mass spectrometer.

Copper tube samples were also extracted in the Dissolved and Noble Gas Lab. Water was transferred from the copper tubes to 500 cc stainless steel flasks under high-vacuum. While still under vacuum, gases were extracted, collected, and sealed in 60 cc stainless steel flasks for analysis on the mass spectrometer line consisting of a Stanford Research System (SRS) – Model RGA 300 quadrupole mass spectrometer for the measurement of Ne, Ar, Kr, and Xe, and a Mass Analyzers Products – Model 215-50 Magnetic Sector Mass Spectrometer to measure ^{3}He and ^{4}He. Recharge temperature and excess air were computed for each site using the closed-system equilibration model (CE) described in Aeschbach-Hertig and Solomon (2013).

Carbonate alkalinity (as $CaCO_3$) was measured at the University of Utah using a Metrohm 905 Titrando titrator automated with the 814 USB Sample Processor. Remaining ions were analyzed using a Metrohm 883 Basic IC plus ion chromatograph (IC). Prior to analysis on the IC, samples that were not filtered during collection, were filtered in the laboratory using a 0.45 μm polypropylene membrane filter. For dissolved silica analysis, 3 mL of each filtered sample was placed into a separate vial with 75 μL of Trace Metal Grade (TMG) hydrochloric acid. These were analyzed by Inductively Coupled Plasma Mass Spectrometry (ICP-MS), also at the University of Utah.

3.3 Chemical Hydrograph Separation

The West Fork Gage – the site of the continuous discharge and SC record – was located downstream of the Vat Diversion (Figure 1). The percent difference between this continuous SC record and several discrete SC measurements made at a site just upstream of the dam was compared to the continuous discharge record at the West Fork Gage (Figure 3). The resulting relationship was used to estimate the continuous SC record above the diversion using daily Vat Diversion records obtained from the Central Utah Water Conservancy District (CUWCD) for the period from March 14, 2014 – March 13, 2015 (Appendix A). In April 2014, several snowmelt samples were collected along the West Fork between these two stream sampling locations in order to characterize the runoff end-member SC. Ultimately, daily baseflow discharge was estimated for 2014 to 2015 at each of the two stream locations using the chemical mass balance approach described in Miller et al. (2014).

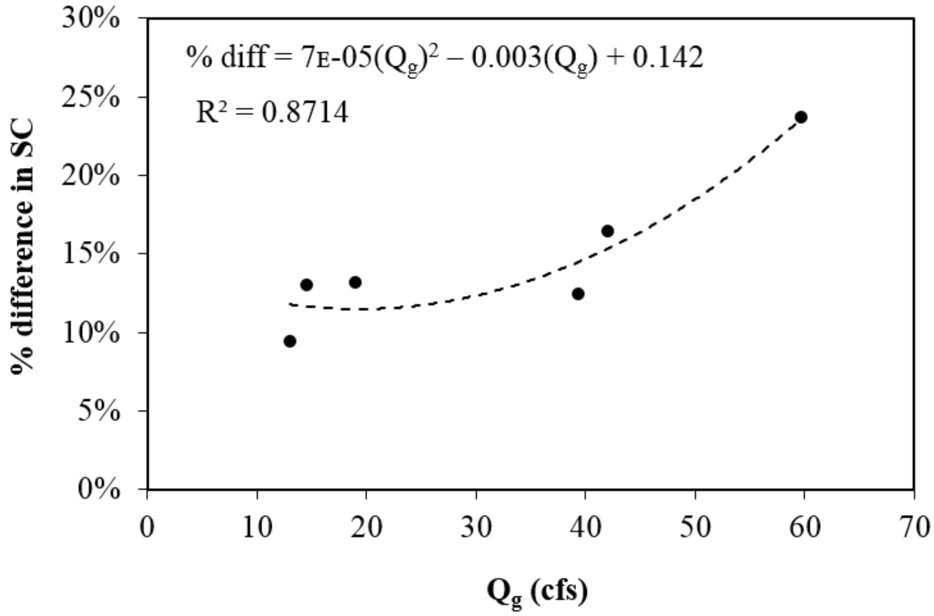

Figure 3. Continuous stream specific conductivity as a function of discharge. The percent difference in discrete SC measurements made above the diversion and the continuous SC at the West Fork Gage is presented on the y-axis. The continuous discharge at the gage (Q_g) is on the x-axis. This was used in the chemical hydrograph separation analysis to estimate the continuous SC record for the stream above the Vat Diversion.

3.4 Lumped Parameter Modeling

3.4.1 Groundwater Transport Models

Measured tracer concentrations were evaluated using TracerLPM – a USGS-developed Excel workbook for groundwater transport modeling. TracerLPM allows multiple environmental tracer concentrations to be analyzed simultaneously in order to determine the age distribution that most appropriately fits the chosen lumped parameter model (LPM) (Jurgens et al., 2012). Initially, two different LPMs were used to evaluate the transit time distributions of West Fork springs; these were the piston-flow model (PFM) and the exponential mixing model (EMM).

The PFM is the simplest LPM and assumes tracer concentrations are confined to a single flowpath from recharge to discharge, both of which are treated as distinct, point locations relative to the overall length of subsurface transit (Jurgens et al., 2012). Therefore, this model does not account for the possibility of mixing or dispersion (Jurgens et al., 2012). Exit age distributions are calculated from tracer concentrations that are assumed to only represent the amount of time the tracer was confined to the subsurface, i.e., the transit time of the water contained in that individual flowpath. The EMM assumes that recharge is uniformly distributed across the areal extent of the water table up to the discharge location (Jurgens et al., 2012). In this case, young and old water – entering the system from both near, and far – are mixed when flowpaths converge upon discharging the system.

A third LPM – the exponential piston-flow model (EPM) - was also assessed in this study in order to account for the possibility of recharge being more concentrated at higher elevations, and less water infiltrating to the depth of the water table near the main channel.

The EPM has an additional parameter referred to as the EPM ratio, which is defined as the ratio of the water table (length) directly recharged by infiltrating water to the extent of the water table (length) that is not being recharged (Figure 4) (Jurgens et al., 2012). As a result, this ratio controls the degree to which the age distribution varies between being purely exponential (EPM ratio = 0), and predominantly piston-flow (EPM ratio > 5) (Jurgens et al., 2012). The EPM provides the most objective characterization of the age distribution at each site.

3.4.2 Unsaturated Zone Travel Time

In order for age-dating with environmental tracers to be accurate, factors affecting gas exchange with the atmosphere must be addressed appropriately. One of these factors is travel time through the unsaturated zone (UZ). The degree to which ^{3}H, ^{3}He, SF_6, and CFCs record transit in the unsaturated zone is not the same. However, the default in TracerLPM is to assume that all tracers start recording time at the water table; therefore, it neglects the effect that UZ transport may have had on certain tracer input concentrations.

For ^{3}He and SF_6, the default in TracerLPM is reasonable; we can assume that these tracer concentrations only provide a record of saturated zone transport. Helium-3 has low solubility and it is likely that any ^{3}He produced in the UZ from ^{3}H-decay is lost to the atmosphere (Rueedi et al., 2005). SF_6 also has a relatively low solubility; as a result SF_6 concentrations may remain close to equilibrium with the atmospheric concentration prior to penetrating the water table (Plummer et al., 2006).

Tritium and CFCs behave differently than ^{3}He and SF_6. As a hydrogen isotope, ^{3}H is part of the water molecule and infiltrates the ground surface with precipitation

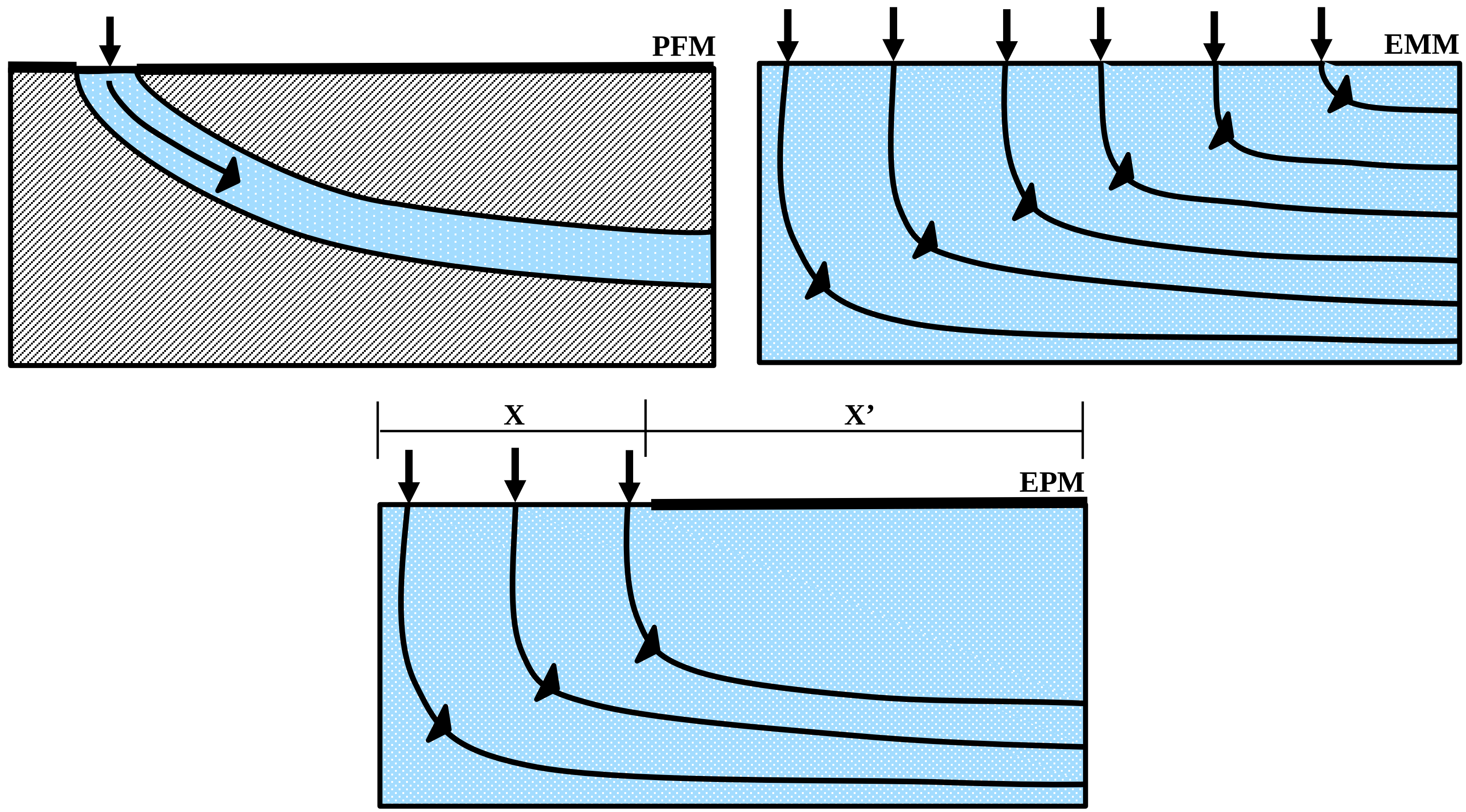

Figure 4. Box models of primary LPMs (Jurgens et al., 2012). The PFM (upper left) describes the most simplistic view of groundwater transport in which water travels from a recharge location to a discharge location without the potential for mixing, or dispersion (Jurgens et al., 2012). The EMM (upper right) accounts for the possibility of more spatially distributed recharge and the mixing between young and old water that occurs upon discharging the system. The EPM (lower) describes a system that is some fraction of piston-flow and exponential mixing (Jurgens et al., 2012). This variability between PFM, and EMM, dominance is controlled by the EPM ratio (X’/X). When X’/X > 5, piston-flow is considered to be the representative transport model. Purely exponential mixing is represented by an EPM ratio of 0.

(Zoellmann et al., 2001; Schwientek et al., 2009). Therefore, it records both unsaturated and saturated zone transport. CFCs also record time in the UZ, perhaps to a lesser extent than ^3H but more than SF_6 or ^3He (Cook and Solomon, 1995). Similar to SF_6, diffusion dominates CFC transport through the vadose zone (Schwientek et al., 2009), but CFCs are more soluble than SF_6, and are therefore less likely to exchange with surrounding atmospheric gases (Plummer et al., 2006). Cook and Solomon (1995) reported that for a thicker UZ (~ 30 m thick), CFC apparent ages may be as great as 20 years older than those estimated by other tracer methods such as $^3H/^3He$. Furthermore, the turnover in the atmospheric curves for CFCs creates an additional apparent lag time that does not exist for SF_6 because its concentration in the atmosphere is still increasing. The fact that SF_6 and CFCs have different solubilities and diffusion coefficients, as well as dissimilar atmospheric curves, is presumed to give rise to differences in the transit times determined from each of these tracers.

When modeling each individual spring, an UZ travel time of 0 years was initially assigned to each of the tracers (^3H, ^3He, SF_6, CFC-11, CFC-12, CFC-113). For each subsequent model run, the UZ travel time assigned to ^3H and CFCs was increased by 2-5 years; the UZ travel time for ^3He and SF_6 was set to 0 years for all model runs with the assumption that the UZ lag time for these two tracers is minimal. For most sites, 10 to 20 different UZ travel times were tested for ^3H and CFCs, ranging from 0 to 35 years.

4 RESULTS AND DISCUSSION

4.1 Chemical Hydrograph Separation

The estimated baseflow end-member SC was ~ 520 µS/cm at the West Fork Gage and ~500 µS/cm above the Vat Dam. A value of 33 µS/cm was determined to be representative of the runoff component at both sites. For the duration of the year when no water was being diverted, baseflow discharge was determined to be slightly higher at the West Fork Gage than at the site above the diversion (Figure 5). However, during snowmelt conditions, when Vat diversions were actively occurring, baseflow discharge was considerably greater at the upstream location than at the gage site (Figure 5).

The annual volume of total discharge measured at the gage was ~2.00 x 10^7 m^3. Approximately 83% of this total volume, or 1.66 x 10^7 m^3 (18.6 cfs), was estimated to be baseflow. The annual volume of discharge measured above the diversion was ~2.09 x 10^7 m^3, with 73% of this volume (1.52 x 10^7 m^3) estimated to be baseflow. The annual baseflow discharge value at the West Fork Gage was used as the representative baseflow volume for the watershed as a whole since this value was obtained using measured discharge and SC, rather than estimated values.

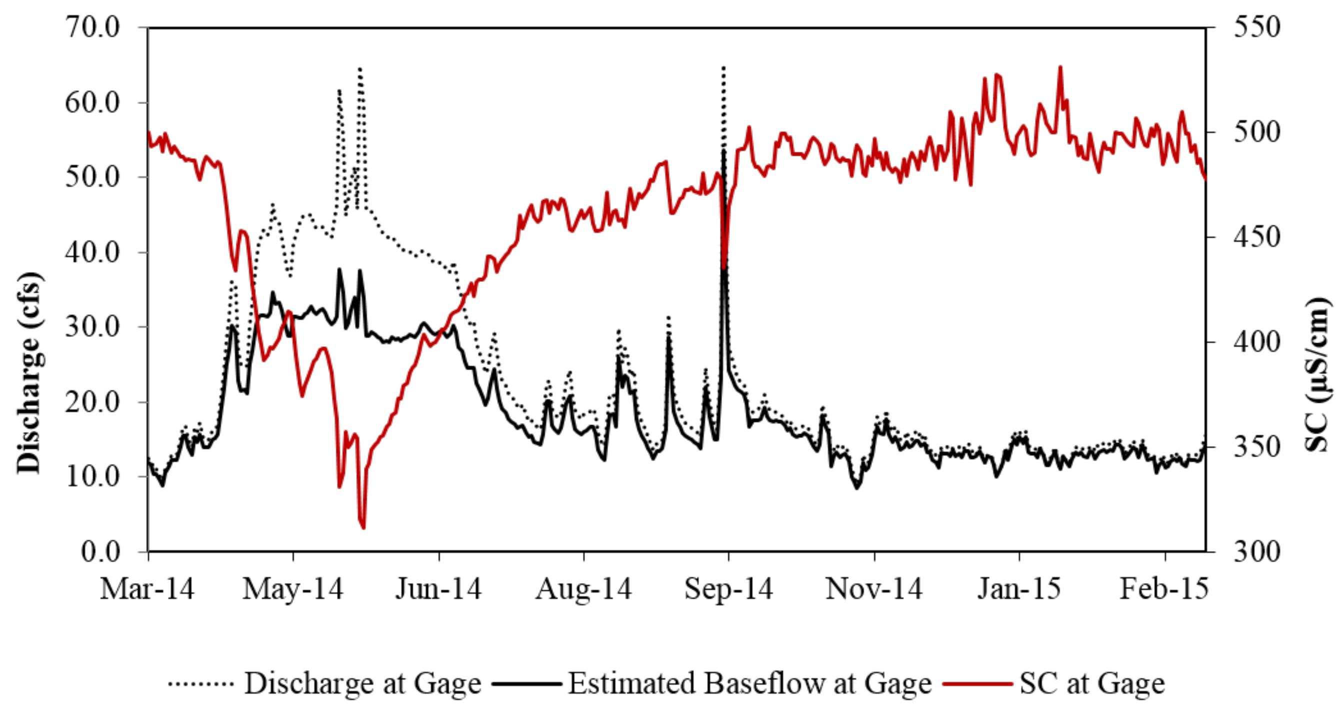

Figure 5. Chemical hydrograph separation analysis. The total stream discharge (dotted black line) and the continuous SC record (solid red line) measured at the West Fork Gage is shown on the above plot. The fraction of this total measured discharge at the Gage that was estimated to be baseflow was calculated using the chemical mass balance approach described in Miller et al. (2014) and is provided by the solid black line.

4.2 Volatile Tracer Results

4.2.1 Laboratory Analysis

Raw tracer data and dissolved gas results for West Fork springs are presented in Table 1. All sites have relatively high ^{3}H, SF_6, and CFC concentrations, indicating predominantly modern-aged (post-1950) water. Recharge temperatures determined from dissolved gas analysis are between 0 and ~3°C for high-elevation springs and range from ~2 to nearly 9°C at lower elevation, near channel, springs. These results are consistent with expectations - colder water is recharging higher elevation springs, whereas lower-elevation locations have the potential to receive either lower-elevation recharge or higher-elevation recharge that has been warmed by more prolonged subsurface transit.

4.2.2 TracerLPM Analysis

TracerLPM EPM-derived ages, UZ travel times, RMS errors, and EPM ratios are provided in Table 2. The decision to rely on the EPM results (rather than PFM, or EMM results) was made as a result of the preliminary tracer-tracer plots provided in Figure 6 that revealed the age distribution at some West Fork springs was more likely exponential mixing, while at other sites age distributions were more appropriately modeled by piston-flow.

Most of the high-elevation, and low-elevation, spring discharge dated in this study were determined to be approximately 30 years old (Table 2). The exceptions were two low-elevation, near-channel, springs with ages of 59 ± 16 years (*South Side Spring #1*) and 115 ± 29 years (*North Side Spring #1*), as well as one low-elevation spring (*LWFDS01*) and one high-elevation spring (*Upper Spring B*) each with a mean age of ~3 years. The

Table 1. SF_6, CFCs, and $^3H/^3He$ Data for West Fork Springs

Recharge temperature and excess air were computed from noble gas concentrations using the closed-system equilibration (CE) model (Aeschbach-Hertig and Solomon, 2013). Salinity was measured using a Hydrolab Multiprobe. Tritium (^3H), tritiogenic helium (^3He), SF_6 , and CFCs were used for lumped-parameter modeling to determine apparent ages. The approximate uncertainties are provided for ^3H and ^3He. Uncertainties in recharge temperature and excess air were not explicitly evaluated for each sample but are approximately ± 1.5 °C and ± 0.5 mL/kg, respectively. The measurement uncertainty for salinity is ~ 5%, and for SF_6 and CFCs it is ~ 3%.

	Site	Rech. Temp. (°C)	Excess Air (mL/kg)	Salinity (‰)	χ^2 *	^3H (TU)	Trit. ^3He (TU)	SF_6 (pptv)(2)	CFC-11 (pptv) (2)	CFC-12 (pptv) (2)	CFC-113 (pptv) (2)
High-Elevation Springs	LWFDS01	2.0	1.7	0.16	0.07	7.0 ± 0.2	1.1 ± 0.2	6.8	283.2	445.0	66.6
	LWFDS05	0.9	1.1	0.16	0.05	6.8 ± 0.2	5.2 ± 0.3	5.2	183.2	424.2	32.3
	LWFDS07	0.0	2.6	0.23	0.20	6.3 ± 0.2	11.5 ± 0.4	4.6	374.9	326.4	69.5
	WFDS08	2.0	0.5	0.09	0.19	7.2 ± 0.3	1.5 ± 0.3	6.1	201.3	421.7	49.4
	WFDS09	0.0	1.2	0.29	0.00	6.2 ± 0.2	5.4 ± 0.3	5.5	241.4	383.4	51.2
	WFDS12	0.0	0.0	0.20	0.24	7.5 ± 0.4	2.5 ± 2.0	5.7	156.5	338.0	37.4
	WFDS13	0.0	1.0	0.31	0.01	7.2 ± 0.3	23.7 ± 6.4	3.5	307.1	240.7	43.7
	New Spring #4	2.7	1.4	–	2.86	7.1 ± 0.3	6.8 ± 0.4	7.0	170.5	408.1	32.6
	Five Suns Spring	0.0	1.2	–	2.09	6.7 ± 0.3	9.0 ± 3.3	4.7	128.2	302.6	33.0

Table 1. continued

	Site	Rech. Temp. (°C)	Excess Air (mL/kg)	Salinity (‰)	χ^2 *	^3H (TU)	Trit. ^3He (TU)	SF_6 (pptv)(2)	CFC-11 (pptv) (2)	CFC-12 (pptv) (2)	CFC-113 (pptv) (2)
Low-Elevation Springs	W.F. Lower Spring	4.9	0.8	0.33	9.80	6.4 ± 0.2	2.5 ± 0.3	6.4	200.7	462.1	45.5
	FR050 Spring	6.2	1.1	0.44	9.27	5.0 ± 0.2	7.6 ± 0.4	2.8	117.2	259.5	26.0
	W.F. Upper Spring	4.3	1.1	0.29	10.85	6.5 ± 0.2	1.4 ± 0.2	6.2	215.9	507.1	48.2
	WFDS10	4.7	0.0	0.10	1.84	8.6 ± 0.4	0.7 ± 0.2	7.2	206.6	395.7	46.6
	WFDS14	4.1	0.2	0.26	0.02	4.4 ± 0.2	3.0 ± 0.2	5.7	203.5	413.8	48.2
	WFDS19	3.9	2.9	0.45	0.27	5.4 ± 0.2	11.0 ± 4.3	2.4	101.4	206.1	20.9
	WFDS19 REP(1)	—	—	—		—	—	2.3	135.7	291.3	30.4
	New Spring #1	7.7	1.5	—	15.94	6.5 ± 0.3	17.2 ± 0.6	3.7	95.5	271.3	24.7
	New Spring #2	7.8	1.8	—	19.31	6.5 ± 0.4	15.6 ± 0.7	3.5	101.8	291.9	27.0
	New Spring #3	7.8	1.5	—	3.25	7.0 ± 0.3	15.5 ± 0.5	6.8	206.0	507.4	47.7
	N. Side Spring #1	2.5	0.4	—	0.20	6.1 ± 0.2	-0.1 ± 1.3	8.4	23.6	303.5	9.1
	S. Side Spring #1	2.4	0.7	—	1.94	1.0 ± 0.1	7.6 ± 1.8	0.8	36.1	107.8	8.0
	Upper Spring B	8.7	1.0	—	6.97	6.5 ± 0.2	-1.8 ± 1.2	8.8	194.0	548.3	62.6

(1) *WFDS19 REP* is the field duplicate of *WFDS19*. The *WFDS19 REP* tritium sample failed during analysis on the mass spectrometer and a *WFDS19 REP* dissolved gas sample was not collected.
(2) SF_6 and CFC concentrations are given in equivalent air concentrations (parts per trillion by volume).
* χ^2 is the sum of the (error weighted) differences between modelled and measured noble gas concentrations (Aeschbach-Hertig and Solomon, 2013)

Table 2. Selected LPM Data for West Fork Springs

EPM TracerLPM-derived ages, EPM ratios, unsaturated zone (UZ) travel times, and RMS errors for the 21 springs sampled within the West Fork watershed. SF_6, ^3H, ^3He (tritiogenic), CFC-11, -12, and -113 tracer concentrations were used at all sites for model optimization unless otherwise noted. Elevation above sea level, discharge, and dissolved silica concentrations, are also provided.

	Site	Elevation (masl)	Age (years)	EPM ratio[1]	UZ travel time (years)	RMS Error (%)	Discharge[2] (cfs)	Si (ppm)
High-Elevation Springs	LWFDS01	3030.0	2.7	0	0	5.0	0.031	3.3
	LWFDS05	2914.8	32.1	≥ 100	22	4.0	0.043	4.3
	LWFDS07	2911.8	27.6	0	19	10.2	0.008	3.9
	WFDS08	2973.3	28.5	≥ 100	25	5.8	0.022	16.4
	WFDS09	2773.1	28.1	≥ 100	17	2.7	—	5.2
	WFDS12	2794.7	32.1	≥ 100	26	5.7	0.009	15.8
	WFDS13	2688.0	32.4	≥ 100	10	12.5	0.005	9.7
	New Spring #4	2813.0	32.6	0	26	3.5	0.170	5.42
	Five Suns Spring	2541.1	32.8	≥ 100	18	7.5	0.654	12.9

Table 2. continued

	Site	Elevation (masl)	Age (years)	EPM ratio[1]	UZ travel time (years)	RMS Error (%)	Discharge[2] (cfs)	Si (ppm)
Low-Elevation Springs	W.F. Lower Spring	2443.3	27.4	≥ 100	21	3.1	—	12.47
	FR050 Spring	2327.8	33.9	≥ 100	15	8.7	—	14.4
	W. F. Upper Spring	2445.4	27.5	≥ 100	23	5.3	0.013	—
	WFDS10	2536.9	28.2	≥ 100	26	5.7	0.016	6.7
	WFDS14	2472.2	28.5	≥ 100	19	1.8	0.057	6.9
	WFDS19	2354.0	38.6	≥ 100	17	8.8	0.144	7.4
	New Spring #1	2436.6	33.4	≥ 100	15	9.6	0.424	9.47
	New Spring #2	2436.9	36.8	≥ 100	16	10.2	0.017	9.53
	New Spring #3	2463.1	29.8	0	20	4.8	0.040	7.09
	N. Side Spring #1*	2249.4	115.0	0	25	25.6	0.069	8.4
	S. Side Spring #1	2269.2	59.0	≥ 100	23	26.4	0.322	6.9
	Upper Spring B*	2449.4	2.7	0	0	6.6	0.013	7.91

* ^3He (tritiogenic) was not used in model optimization because negative values were returned from noble gas analysis.
(1) An EPM ratio ≥ 5 is representative of purely piston-flow. EPM ratios were generally far greater than 100 (ranging from 100 to 5.5 x 10^{13}). Only six sites yielded EPM ratios of 0, which is characteristic of purely exponential mixing.
(2) Discharge measurements were made using a 3 in. Parshall Flume, a bucket and stopwatch or flow meter. Discharge was not measured at *WFDS09, West Fork (W.F.) Lower Spring*, and *FR050 Spring*; these sites were not suitable for these measuring techniques.

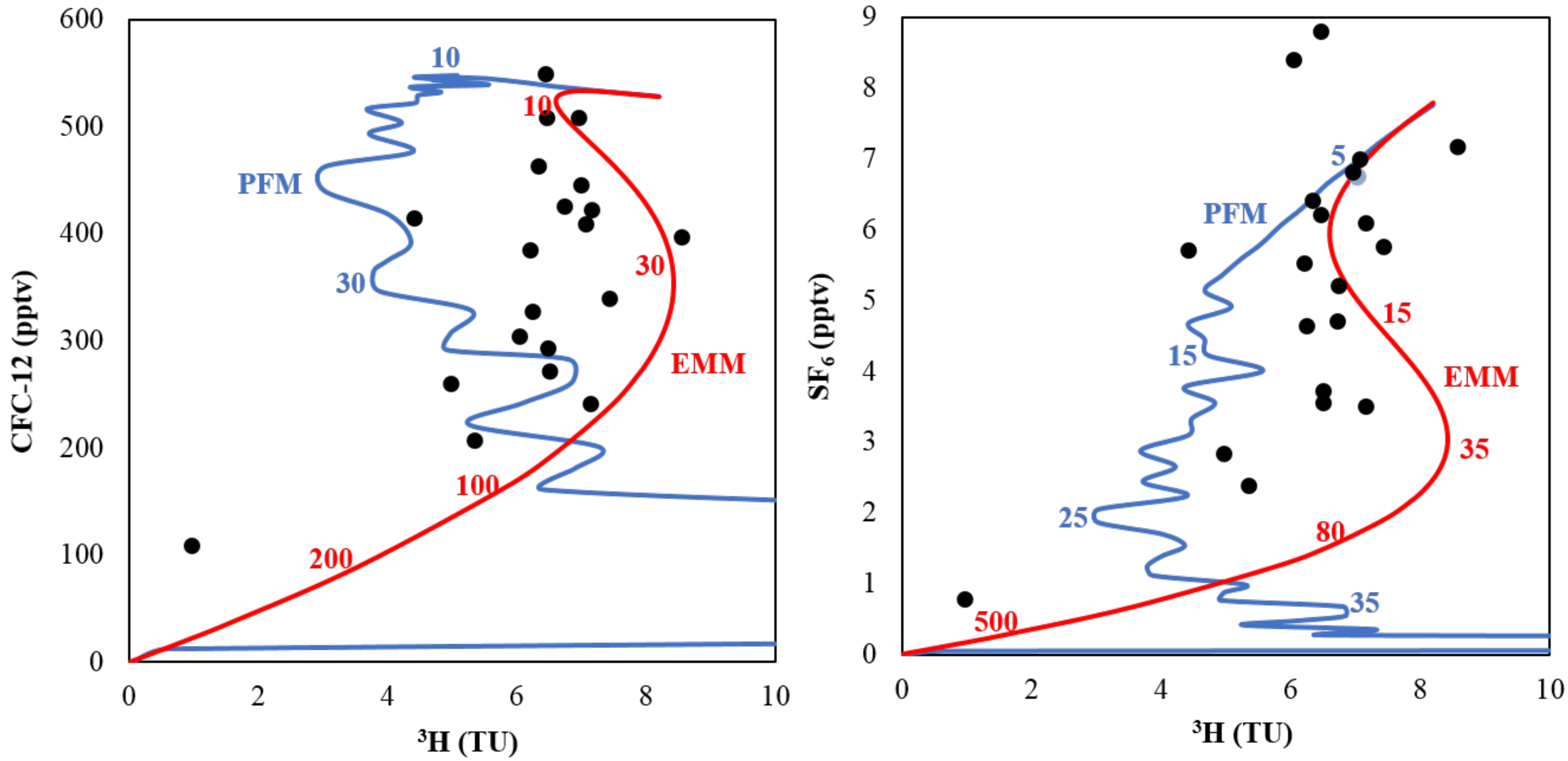

Figure 6. Tracer-tracer plots of CFC-12 versus ^3H (left) and SF_6 versus ^3H (right). West Fork spring concentrations are denoted by black circles and generally plot between the PFM and EMM modeled concentrations provided by the blue and red lines, respectively. Values next to each LPM represent the ages (in years) corresponding to modeled concentrations for that given LPM.

geographic distribution of recharge and hydrogeologic factors affecting the rate of infiltration and transport through the subsurface provide possible explanations for why these outliers exist. However, a limited understanding of the precipitation patterns and geology in the region make it difficult to draw definitive conclusions.

Based on the geologic maps of the region, *South Side Spring #1* and *North Side Spring #1* are located in the Ankareh Formation which is described as fine-grained sandstone and mudstone (Bryant, 2010). It seems likely that these two near-channel springs would have older water (as a result of longer flowpaths) than *Five Suns Spring* and *WFDS14* which are located in the same formation but at higher elevations. However, *Five Suns Spring* and *WFDS14* were dated at ~33 ± 2.5 years, and ~29 ± 0.5 years, respectively. As a result, the overall hydrologic characteristics of this geologic unit are considered to be a less likely cause for the older spring ages near-channel compared to the actual length of the flowpaths, that is, heterogeneity within the formation itself probably is more important (i.e., preferred flowpaths along fractures, more permeable lihologic units, etc.). In addition, SF_6 and CFC tracer fits for *South Side Spring #1* and *North Side Spring #1* were particularly poor which resulted in the highest RMS errors reported for any of the sites. These older ages were primarily controlled by ^3H concentrations, and are therefore considered to be less reliable than the other spring ages reported in the study.

Similar questions arise for the two youngest springs in the dataset - *LWFDS01* and *Upper Spring B*. It's possible that the young age of 2.7 ± 0.1 years for *LWFDS01* (the highest elevation spring included in the study) can be attributed to this spring's proximity to the watershed boundary (Figure 1). Subsurface transit time is at a minimum because discharge is occurring fairly close to recharge. *Upper Spring B*, however, is a low-elevation, near-channel spring located in the vicinity of *New Spring #1, #2*, and *#3*, and *West Fork Lower Spring*, and the approximate age for these springs is 32 ± 5 years. Once again, the limited geologic understanding of the region does not provide a clear explanation for why *Upper Spring B* is significantly younger than these neighboring sites, but it is reasonable to assume that preferential groundwater flowpaths are responsible for faster transit times even within the same lithologic unit. Another possibility is that *Upper Spring B* is simply a lower elevation discharge location of groundwater that was initially discharged at a higher elevation, thus permitting gas reequilibration before reinfiltrating the subsurface.

EPM ratios for 6 of the West Fork springs is 0, signifying exponential mixing, whereas the remaining 15 sites have EPM ratios ≥ 100 which indicate a purely piston-flow transport model. It is understandable that a majority of the higher-elevation springs are more appropriately modeled by piston-flow as a result of the limited area over which recharge likely occurs. However, for the lower-elevation springs, the PFM lumped-parameter model also best fits the tracer data. This result is somewhat unexpected given the much greater length of water table available for recharging water to infiltrate prior to discharging at these lower-elevation locations. The oldest spring in the study (*North Side Spring #1* at ~115 years) is more appropriately modeled by exponential mixing which is understandable given its proximity to the main channel. However, it seems more likely that 115 year old water would have been recharged from a distant, and more confined, recharge area represented by piston flow transport. As previously mentioned, the higher RMS error associated with tracer fits for this site make it a less reliable result in general. This overall lack in correlation between lumped-parameter models and spring locations is consistent with EPM-determined ages which also show minimal correlation with spring location. Again, lithologic heterogeneity, and the possibility for preferential flowpaths existing as a result of subsurface geology, are likely most responsible for controlling groundwater transport in the West Fork watershed.

On the contrary, there are several exceptions for which lumped-parameter model and spring location (and recharge temperature) are comparable. Of the springs included in this study, *New Spring #3* and *Upper Spring B* have the warmest recharge temperatures (7.8 and 8.7°C, respectively). As expected, these are low-elevation springs which have purely exponential mixing. Similarly, the fact that the two youngest springs in the study (*LWFDS01* and *Upper Spring B*) are modeled by exponential mixing is also consistent with expectations; recharge from nearby is contributing a significant fraction of younger water to spring discharge in addition to the older water recharged at more distant locations.

An initial plot of SF_6 vs. CFC-12 for all West Fork springs revealed that measured SF_6 concentrations were greater than model expectations for corresponding CFC concentrations, or that measured CFC concentrations were less than those expected by the LPMs – evidence that CFCs may be recording additional transit time not recorded by SF_6 (Figure 7), or that there is a terrigenic source of SF_6 within the West Fork watershed similar to that described in Koh et al. (2007). However, a secondary source of SF_6 is considered less likely because measured SF_6 concentrations from the springs were generally less than atmospheric SF_6 concentrations (~8 pptv) (Table 1). Furthermore, SF_6-determined ages are highly comparable to those determined from $^3H/^3He$ dating. By adding an UZ travel time of ~ 18 years to CFCs (as well as ^3H) in TracerLPM this discrepancy between tracers was apparently corrected (Figure 7). This confirms the need to account for UZ travel times

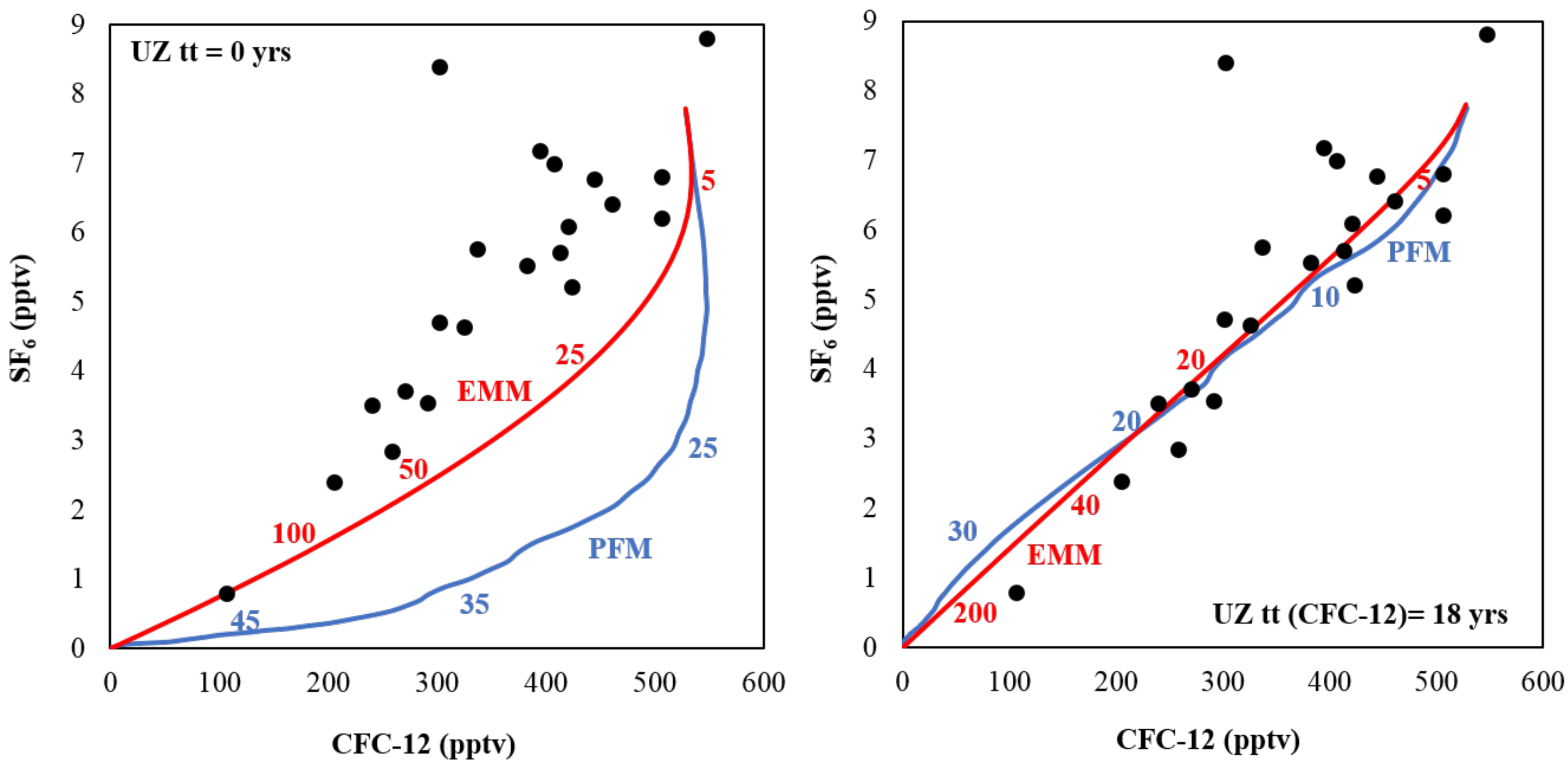

Figure 7. Tracer-tracer plots of SF_6 versus CF-12 for 0 (left) and 18 years (right) UZ travel time. The PFM and EMM modeled concentrations are provided by the blue and red lines, respectively. Values next to each LPM represent the ages (in years) corresponding to modeled concentrations for that given LPM. West Fork spring concentrations (denoted by black circles) generally have greater SF_6 concentrations than modeled expectations with 0 years UZ travel time. Tracer fits are improved when it is assumed that CFC-12 is recording additional time in the subsurface (~ 18 years in the UZ).

separately for each tracer included in model parameterization. The UZ travel times reported in Table 2 are those that resulted in the lowest root mean squared (RMS) error for a given model output. For two of the West Fork springs it was determined that an UZ transit time of 0 years provided the best-fit between measured, and modeled, tracer values (Table 2). For all other springs, the average UZ travel time was ~ 20 ± 6 years.

4.3 West Fork Groundwater Assessment

4.3.1 Study Assumptions

Several assumptions were made in this study that deserve careful consideration before assessing groundwater storage within the West Fork watershed: (1) Is the baseflow estimate obtained from the chemical hydrograph separation truly representative of groundwater discharge within the watershed? (2) Can springs provide an accurate characterization of the discharging groundwater in terms of age and chemistry?; (3) If so, what fraction of total baseflow volume needs to be sampled from spring sites in order to characterize watershed groundwater as a whole?

In regards to the first question, baseflow estimates do not necessarily equate to total groundwater discharge. In reality, baseflow is simply a measure of the groundwater component that contributes to streamflow. As seen in the West Fork watershed, the river channel is not the only groundwater discharge location. Using baseflow as a direct proxy for groundwater discharge fails to account for the discharge occurring at seeps and springs. However, it is considered to be a decent approximation because, during cool dry baseflow conditions, discharge at seeps and springs eventually reaches the main West Fork channel.

The answer to question two is largely related to question three. Springs are locations where groundwater flowpaths converge and intersect the land surface. As a result, it can be assumed that spring water provides a good representation of discharging groundwater within (at least) a portion of the total watershed area – the area over which that groundwater was recharged. Therefore, spatially representative spring sampling may be more important than maximizing the total volume of spring water sampled. In this study, the combined discharge from the 18 springs with discharge measurements only accounts for approximately 11% of the total annual estimated baseflow of the stream, but these springs are distributed throughout the watershed – both close to, and far from, the West Fork, and ranging from headwater to down-channel locations. Also, the flow-weighted average ^3H concentration of these 18 springs is 5.7 TU. This compares quite closely to the average of the five baseflow stream ^3H measurements (5.6 TU), indicating that the selected springs adequately represent groundwater in the watershed.

4.3.2 MTT and Storage

The flow-weighted mean age was calculated based on all sites at which discharge was measured (Table 2). This provided an approximate groundwater MTT of 40 years for the West Fork watershed. Using Eq. (1), and assuming that the annual average baseflow value estimated from the chemical hydrograph separation analysis (1.66 x 10^7 m^3/year) is representative of groundwater discharge rates, the volume of stored groundwater (V) was was determined to be ~6.5 x 10^8 m^3. Using an estimated porosity of 0.15 - the mean for the range of porosities provided by Freeze and Cherry (1979) for limestone and sandstone - the total volume of the saturated zone containing this mobile water is ~4.4 x 10^9 m^3. This translates to an approximate saturated zone thickness of 24 m, or ~ 0.09 m/year of water recharging the groundwater system that ultimately discharges as West Fork streamflow. It is important to note that this saturated zone thickness is particularly sensitive to the assigned value for porosity. For example, if the porosity within the West Fork watershed is considerably lower at 0.05, then the saturated zone thickness could be as great as ~ 70 m; if the average porosity is significantly higher, around 0.30, then the saturated thickness could be closer to ~12 m.

Nevertheless, the active circulation depth of groundwater throughout the watershed is fairly shallow at 24 m (or 12-72 m) in comparison to the thicknesses of the permeable geologic units within the watershed (i.e., ~230 m-thick Preuss Sandstone, ~240 m-thick Twin Creek Limestone, ~400 m-thick Nugget Sandstone, and ~500 m-thick Ankareh). This is attributed to the presence of less permeable shales and siltstones in the more shallow geologic units, especially in the Preuss and Twin Creek Formations.

The calculated equivalent recharge rate of 0.09 m/year ranges between ~10% of the annual precipitation falling on the uppermost headwaters to nearly 24% of the annual precipitation reported for the lower half of the West Fork. For comparison, McMahon et al. (2011) determined that the median recharge rate for the Basin and Range aquifer system in western Utah and Nevada is approximately 0.19 m/year; this was based on 24 different sites at which recharge rates ranged from ~ 0.04 m/year to as much as 1.2 m/year. Average precipitation in the more mountainous regions of the Basin and Range varies from ~ 0.5 to 0.8 m/year (Robson and Banta, 1995). The recharge rate provided by Mahon et al. (2011), is ~ 24 – 38% of this annual average precipitation. Robson and Banta (1995), however, suggest a considerably lower value; according to their study, only 5% of precipitation replenishes the Basin and Range aquifer each year since most of the precipitation is lost to evapotranspiration. Nonetheless, these results for the Basin and Range are in good agreement with those determined for the West Fork watershed, especially considering the variability in characteristics such as, the rate of evaporation, fracture density, hill slope, and vegetation density between these two sites.

4.3.3 Cumulative Age Distribution

By utilizing the mean age from each spring (as determined by TracerLPM) an estimate of the cumulative age distribution for the entire watershed was obtained (Figure 8). This cumulative age distribution was constructed by sorting 18 of the 21 springs (the sites at which discharge was measured) by mean age. Discharge measurements from each spring were used to calculate the fraction of total flow from each spring, and plotted as the fraction of flow younger versus the TracerLPM-determined mean age.

Assuming that the sampled volume of spring discharge accurately characterizes the groundwater within the watershed, the cumulative age distribution plot provides a representation of the relative volume of old, versus young, water contained therein. For the West Fork watershed, nearly 80% of the groundwater plots within a narrow age band ranging from 30 to 50 years (Figure 8). For reference, Figure 8 also shows the theoretical curve for an exponential distribution, and for piston flow, for a mean age of 40 years. The observed values plot between these end-member distributions, which is consistent with an exponential piston flow distribution being representative of the entire watershed.

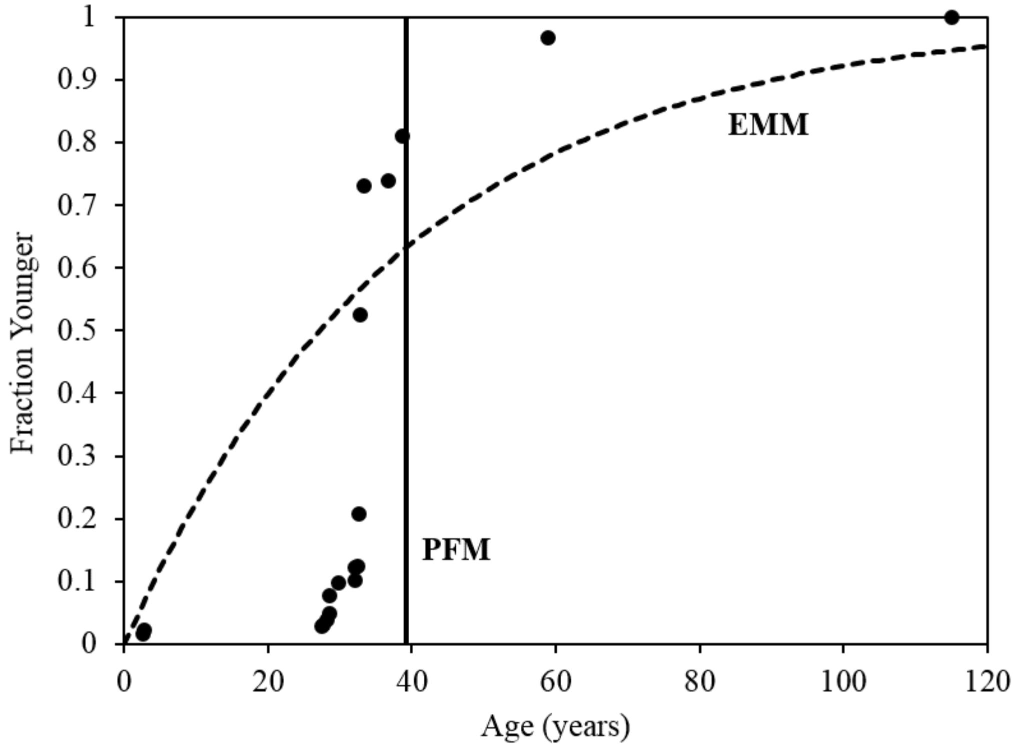

Figure 8. The cumulative age distribution for West Fork watershed according to West Fork springs. The x-axis provides the TracerLPM EPM-derived spring ages, and the y-axis represents the fraction of the total discharge from these springs that is less than a given age (only springs at which discharge was measured is included in this age distribution – *WFDS09*, *West Fork Lower Spring*, and *FR050* are excluded). As expected, the EPM-derived age results plot between the theoretical exponential and piston flow curves. Both of these theoretical curves are displayed with a mean age of 40 years – the groundwater MTT determined for the West Fork.

4.4 Nonvolatile Tracer Results

4.4.1 Major-ion Geochemistry

Major cation and anion concentrations from West Fork springs are provided in Appendix A. Measured spring ion concentrations as related to TracerLPM EPM-determined ages are shown in Appendix B; a correlation to spring age is not apparent for any of the major ions analyzed.

The relationship between spring major-ion geochemistry and location within the watershed (high- versus low-elevation) was also evaluated. Little, or no, correlation exists between spring location and concentrations of magnesium, calcium, sodium plus potassium, or chloride, fluoride, and nitrite plus nitrate (Figure 9). However, the location of the higher elevation springs on the main diamond of the Piper diagram in Figure 9 reveals that these sites generally contain more carbonate and bicarbonate and less sulfate (and chloride) than the lower elevation springs visited in this study. Less chemically evolved water is discharging at higher elevations, which is expected given the proximity of this discharging water to the area over which recharge occurred.

The average age of the West Fork springs (not flow-weighted) is approximately 30 years. Several low elevation piston-flow springs have ages greater than this mean, including *FR050*, *WFDS19*, *New Spring #2*, and *South Side Spring #1* (*North Side Spring #1* was not included in the geochemical analysis due the potential inaccuracy in measured concentrations as indicated by its particularly high percent error in charge balance). As expected, three of these springs have noticeably higher sulfate (and chloride) concentrations than the presumed-to-be younger higher elevation springs. This concept of chemical evolution is also consistent with the LPM interpretation discussed in Section 4.2.2

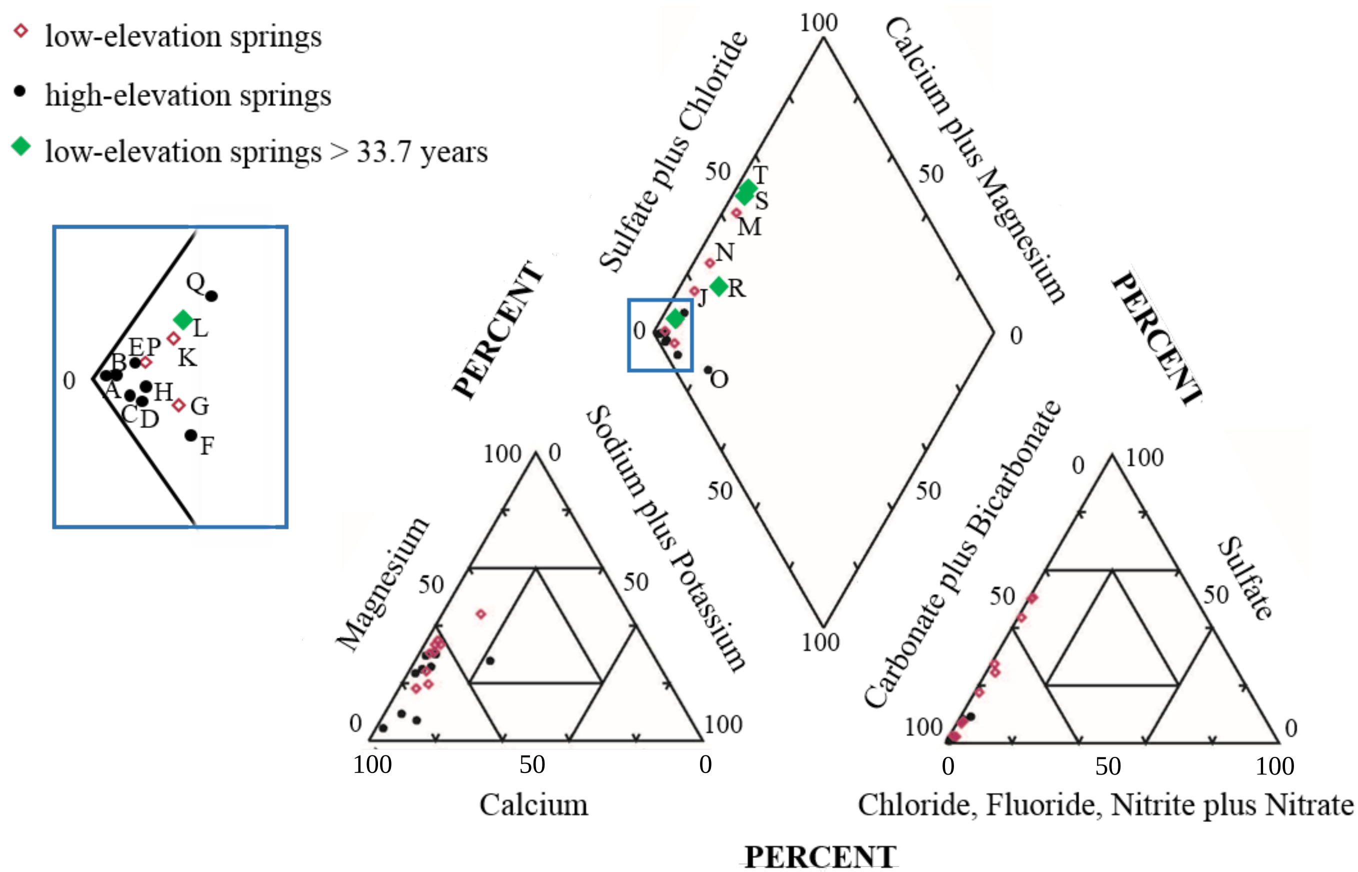

Figure 9. Piper diagram displaying West Fork spring major-ion chemistry in comparison to location within the watershed. High-elevation springs are concentrated in the region representing higher concentrations of carbonate and bicarbonate and minimal amounts of sulfate (and chloride). The mean (not flow-weighted) age of the springs is ~30 years; low-elevation springs older than this mean are denoted by the green diamonds. The letters correspond to the following sampling location names: A = *LWFDS01*, B = *LWFDS05*, C = *New Spring #4*, D = *LWFDS07*, E = *WFDS09*, F = *WFDS08*, G = *WFDS10*, H = *WFDS12*, J = *Upper Spring B*, K = *New Spring #1*, L = *New Spring #2*, M = *New Spring #3*, N = *West Fork Lower Spring*, O = *WFDS13*, P = *WFDS14*, Q = *Five Suns Spring*, R = *South Side Spring #1*, S = *WFDS19*, T = *FR050 Spring*.

in which piston-flow recharge from higher elevations is ultimately discharging to older, lower-elevation springs. In contrast, younger, lower-elevation springs dominated by exponential mixing, e.g., *Upper Spring B*, are less chemically evolved which is consistent with more local recharge (Figure 9). *New Spring #2* (~37 years of age) plots within the cluster of higher elevation sites suggesting that age is not the only factor affecting the extent to which discharging water has chemically evolved. The heterogeneity of the subsurface geology within the West Fork watershed is also an important factor affecting the geochemistry of the discharging water.

4.4.2 Dissolved Silica

Dissolved silica concentrations from each spring (Table 1) were plotted against the age determined using TracerLPM (Figure 10). At this watershed-scale, there is no correlation between dissolved silica (SiO_2) and age. This is contrary to the results reported in Peters et al. (2014) and Morgenstern et al. (2010), suggesting that variations in bedrock lithology within some watersheds is likely too significant to make this silica-age relationship universally applicable. For example, in this study, *WFDS08* and *WFDS12* have relatively high SiO_2 concentrations given their fairly average age. This can at least partly be explained by the proximity of these two springs to the Keetley Volcanics (Figure 2), a silica-rich lithologic unit within the West Fork watershed through which groundwater likely flows prior to discharging at these two sites.

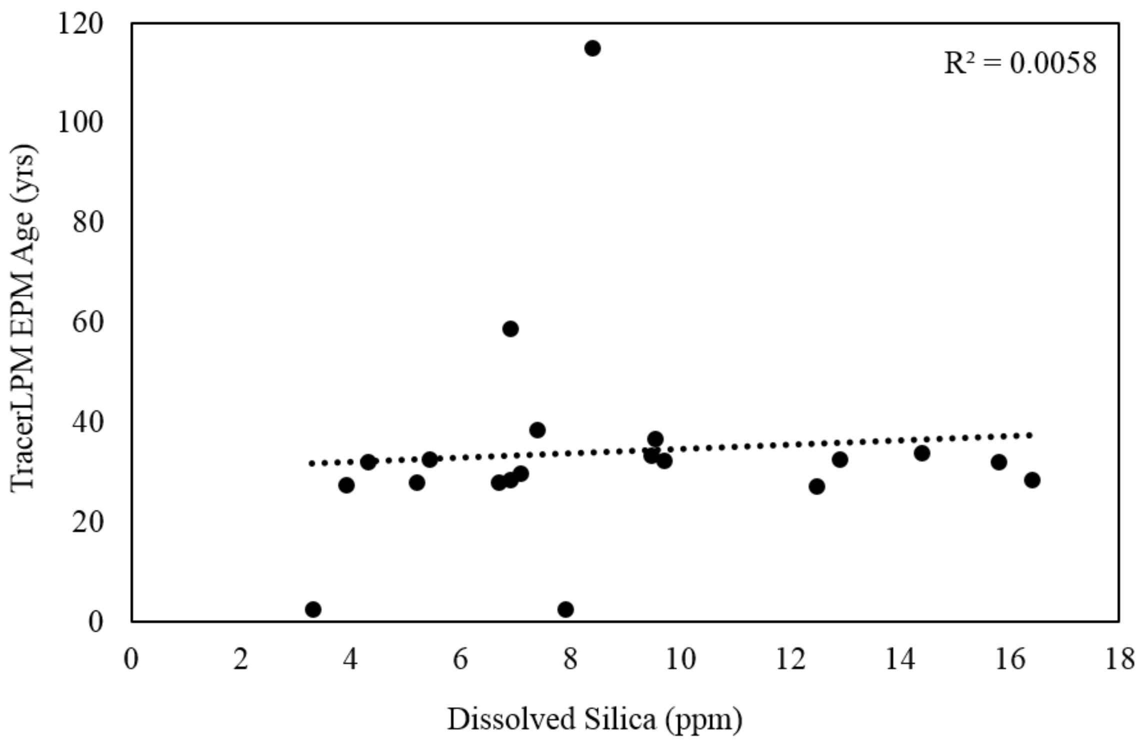

Figure 10. The relationship between TracerLPM EPM-derived ages and measured dissolved silica at West Fork springs. Note: dissolved silica was not analyzed for *West Fork Upper Spring*, and is therefore not included on the above plot. In general, there is no apparent correlation between Si and age within the West Fork watershed – a result attributed to the geologic heterogeneity in a catchment of this size.

4.4.3 Stream Tritium

Baseflow ^3H concentrations, T_B, were calculated using the following mass balance relationship:

$$T_s Q_s = T_B Q_B + T_M Q_M \quad (2)$$

where T_S and Q_S refer to measured stream ^3H concentrations and total stream discharge, respectively; Q_B refers to estimated baseflow discharge from the hydrograph separation analysis; and T_M and Q_M refer to modern ^3H concentrations and the remaining fraction of stream discharge derived from runoff. Calculated T_B values are reported in Table 3 and range between ~4.9 and ~6.6 TU. These calculated values are similar to measured stream concentrations, which is consistent with the high percentage of discharge that was estimated to be baseflow during these sampling times. In general, ^3H values are greater at the upstream site relative to the downstream location, indicating that there is a substantial amount of older water (groundwater) gained throughout the lower reaches of the watershed.

Age determinations from estimated baseflow ^3H concentrations were particularly sensitive to the transit time distribution modeled in TracerLPM (Table 3). The average EMM output age was approximately 98 years, but the PFM output age was significantly less – only 16 years. This discrepancy is attributed to the nonlinear relationship between atmospheric (input) ^3H concentrations and time, and also the fact that present-day atmospheric ^3H has only stabilized in the Northern Hemisphere within the past ~ 10 years.

Additionally, stream ^3H ages were flow-weighted based on the resulting EPM ratios of the TracerLPM analysis of West Fork springs. The MTT for the West Fork watershed

Table 3. TracerLPM Analysis of West Fork Stream Samples

Measured tritium concentrations and discharge at the two stream sampling sites is provided. Baseflow tritium and baseflow discharge were estimated from the chemical hydrograph separation analysis. Baseflow ages were modeled using TracerLPM.

Site	Sample Date	Stream ^3H (TU)	Stream Discharge[(1)] (cfs)	Estimated Baseflow Discharge[(2)] (cfs)	Baseflow ^3H[(3)] (TU)	Baseflow EMM Age (years)	Baseflow PFM Age (years)
West Fork Gage (below Wolf Creek)	10/9/2014	5.6 ± 0.4	19.03	17.56	5.31	107.0	25.5
	1/5/2015	5.3 ± 0.4	15.00	14.17	5.12	111.0	27.0
	2/23/2015	5.1 ± 0.4	13.00	12.39	4.92	116.8	18.1
West Fork above Vat Diversion	10/9/2014	6.7 ± 0.7	10.00	9.27	6.55	73.2	5.0
	2/23/2015	6.1 ± 0.4	6.00	5.73	5.99	84.1	6.6

(1) Discharge below Wolf Creek was provided by the multiprobe meter installed at the West Fork Gage site. Stream discharge above the diversion was taken from CUWCD diversion records.
(2) Discharge and SC measured at the West Fork Gage site were used to estimate baseflow below Wolf Creek. Discrete SC measurements made above the diversion were compared to measured SC at the West Fork Gage in order to estimate continuous SC, and also baseflow discharge, above the diversion.
(3) Baseflow tritium concentrations were calculated using the relationship, $T_sQ_s = T_bQ_b + T_mQ_m$, where T refers to tritium concentrations and Q refers to discharge for the stream (s), for baseflow (b), and for the modern (m) fraction of stream discharge that does not include baseflow. A value of 8.67 TU was used for T_m.

that resulted from this attempt to correct for the variability in transit time distribution was ~ 34 years. While this is in considerably better agreement with the West Fork MTT (40 years) obtained from lumped-parameter modeling of SF_6, CFCs, ^3H, and ^3He (tritiogenic), it would not have been possible without the LPM analysis because the ratio of EMM to PFM groundwater transport would not have been independently discernable. As a result, ^3H alone is currently not a useful nonvolatile tracer for determining groundwater MTT within watersheds with groundwater ages greater than 20 years, at least at similar Northern Hemisphere latitudes where the stabilization of atmospheric tritium has been more recent compared to the Southern Hemisphere.

5 CONCLUSIONS

5.1 West Fork Watershed Susceptibility

SF_6, CFCs, ^3H, and ^3He (tritiogenic) concentrations of 21 springs within the West Fork watershed were analyzed with lumped-parameter models in order to determine the groundwater MTT for the catchment. Spring ages ranged from ~ 3 to 115 years, with the majority of springs dating around 30 years. Lithologic heterogeneity within the watershed, as well as more local variations in the geohydrologic environment, are most likely responsible for the contribution of both young and old water to the system. A MTT for the West Fork watershed of ~ 40 years was calculated as the flow-weighted average of 18 of these 21 spring ages. A chemical hydrograph separation of West Fork streamflow estimated the average annual baseflow volume to be ~1.7×10^7 m^3/year. Assuming steady-state conditions, this proxy for the rate of groundwater discharge within the watershed was used in conjunction with MTT to calculate the volume of mobile stored groundwater within the West Fork Duchesne River watershed. This volume was ~6.5×10^8 m^3, or ~0.09 m/year of recharge over the entire watershed.

From a water resources point of view, the 40-year MTT of groundwater in the West Fork watershed indicates its resiliency to drought. In this region of the U.S, droughts in recent years have typically been less than 10 years in duration (Wilkowske et al., 2003). The expected impact of such droughts on West Fork baseflow is much less than if the MTT was an order of magnitude lower (i.e., years versus decades). In contrast, lasting changes in the rate of groundwater withdrawals, land use, and climate would likely have a profound effect on the West Fork watershed even though these consequences may not be immediately evident.

5.2 Determining MTT Using Nonvolatile Tracers

Under the conditions present in this study, nonvolatile tracers (in-stream major-ion chemistry, dissolved silica, and ^3H) were determined to be ineffective for assessing groundwater MTT. A correlation between chemistry (major-ion concentrations and dissolved silica content) and groundwater age was not apparent, a result attributed to variations in bedrock lithology in the watershed. Additionally, ages determined from stream ^3H concentrations were considerably sensitive to the transit time distribution employed during analysis. This is likely a consequence of both the nonlinear relationship between input ^3H and time at more northern latitudes, as well as the variability in present-day atmospheric inputs.

For these reasons, watershed-scale assessments conducted in the near-future should employ lumped-parameter modeling of multiple environmental tracers to determine groundwater MTT. However, the usefulness of stream ^3H concentrations should be re-evaluated in future decades assuming that atmospheric ^3H continues to stabilize in the Northern Hemisphere. For watersheds like the West Fork in which the majority of the groundwater is approximately 30 years old, stream ^3H sampling (a simpler and less-costly approach than sampling multiple environmental tracers in springs) might provide a viable estimate of groundwater MTT 20-30 years from the present.

APPENDIX A

SUPPLEMENTAL DATA FROM WEST FORK SPRING AND STREAM SAMPLING, GAGE, AND VAT DIVERSION

Appendix A contains supplemental data from springs, and stream locations, sampled within the West Fork watershed. Field parameters and major ion chemistry data from spring sites can be found in the initial pages. Continuous stream data from the West Fork Gage for the period of March 14, 2014 to March 13, 2015 is also included. The final pages present the Vat Diversion records obtained from Central Utah Water Conservancy District (CUWCD) for the March 2014-March 2015 time period.

Table 4. Field Parameters for West Fork Springs

Temperature, specific conductivity (SC), pH, dissolved oxygen (DO), and total dissolved gas pressure (TDG) were recorded during sampling using a Hydrolab Multiprobe. Below, are the final readings taken once all parameters stabilized. A Garmin GPSmap 62s was used to measure elevation. Discharge measurement methods included B = bucket and stopwatch, PF = Parshall flume, or FM = SonTek FlowTracker Handheld Flow Meter.

Site	Sample Date	Elevation (MASL)	Temperature (°C)	SC (µS/cm)	pH	DO (mg/L)	TDG (mmHg)	Discharge (cfs) and Measurement Method	
LWFDS01	7/16/2014	3030.0	3.41	239	6.85	9.71	582	0.031	B
LWFDS05	7/16/2014	2914.8	4.92	249	6.62	7.00	607	0.043	PF
LWFDS07	7/16/2014	2911.8	3.67	352	6.86	3.75	608	0.008	B
WFDS08	7/18/2014	2973.3	4.00	138	5.88	6.35	546	0.022	B
WFDS09	7/16/2014	2773.1	4.75	437	6.66	6.24	621	—	—
WFDS12	7/15/2014	2794.7	4.05	307	6.77	7.28	559	0.009	PF
WFDS13	7/15/2014	2688.0	4.02	477	6.76	2.82	537	0.005	B
New Spring #4	10/17/2014	2813.0	4.72	390	6.95	5.76	611	0.170	PF
Five Suns Spring	10/28/2014	2541.1	3.83	261	7.79	7.67	613	0.654	FM
W.F. Lower Spring	11/26/2013	2443.3	5.17	501	7.16	6.09	565	—	—
FR050 Spring	11/26/2013	2327.8	6.53	668	7.10	5.92	616	—	—
W.F. Upper Spring	11/27/2013	2445.4	4.51	442	7.21	5.84	559	0.013	PF
WFDS10	7/18/2014	2536.9	5.93	152	6.25	8.25	567	0.016	PF
WFDS14	7/18/2014	2472.2	5.52	392	6.84	7.17	578	0.057	PF
WFDS19	7/18/2014	2354.0	6.72	685	6.95	6.67	673	0.144	PF
New Spring #1	10/14/2014	2436.6	5.79	314	6.77	6.16	604	0.424	PF
New Spring #2	10/14/2014	2436.9	5.67	320	6.75	6.51	605	0.017	PF
New Spring #3	10/17/2014	2463.1	4.82	666	7.00	5.01	570	0.040	PF
N. Side Spring #1	10/28/2014	2249.4	8.70	440	7.00	1.20	602	0.069	PF
S. Side Spring #1	10/28/2014	2269.2	8.70	440	7.00	7.50	602	0.322	PF
Upper Spring B	10/17/2014	2449.4	4.17	434	7.01	4.40	532	0.013	PF

Table 5. Major-ion Chemistry of West Fork Springs

Major cation and anion concentrations were analyzed at the University of Utah using a Metrohm 883 IC Basic Plus ion chromatograph. A Metrohm 905 Titrando titrator was used to measure alkalinity as $CaCO_3$. Charge balance error (%) is defined as $\frac{\sum cations - \sum anions}{\sum cations + \sum anions} \times 100$. Ion chemistry was also compared to age to evaluate additional nonvolatile methods for evaluating groundwater MTT. Results of this analysis are presented in Appendix B.

Site	Li^{+} (mg/L)	NH^{4+} (mg/L)	Ca^{2+} (mg/L)	Mg^{2+} (mg/L)	Na^{+} (mg/L)	K^{+} (mg/L)
LWFDS01	–	–	53.253	1.516	1.116	0.447
LWFDS05	–	–	48.573	9.319	1.411	0.488
LWFDS07	0.010	–	56.424	15.834	3.686	2.258
WFDS08	–	–	25.456	1.328	3.217	1.094
WFDS09	0.005	–	77.272	16.333	3.895	0.754
WFDS12	–	–	58.809	3.890	3.094	1.599
WFDS13	0.009	–	54.914	18.496	27.752	1.025
New Spring #4	0.001	–	60.678	16.016	1.839	0.807
Five Suns Spring	–	–	40.527	9.228	3.033	1.457
W.F. Lower Spring	–	–	75.160	24.620	6.052	1.180
FR050 Spring	–	–	99.450	34.030	5.691	1.036
W.F. Upper Spring	–	–	–	–	–	–
WFDS10	0.001	–	25.543	4.247	2.666	0.943
WFDS14	–	–	60.616	16.759	2.951	0.585
WFDS19	0.005	–	104.600	33.516	5.517	0.987
New Spring #1	0.002	–	52.382	7.556	3.258	1.240
New Spring #2	–	–	53.671	7.789	3.306	1.255
New Spring #3	0.010	–	97.961	28.195	6.577	1.088
N. Side Spring #1	0.003	–	41.979	29.928	8.651	0.903
S. Side Spring #1	0.004	–	34.553	20.737	9.552	1.350
Upper Spring B	0.002	–	69.748	14.425	5.142	1.006

Table 5. continued

Site	HCO_3^- (mg/L)	NO_2^- (mg/L)	Br^- (mg/L)	NO_3^- (mg/L)	PO_4^{3-} (mg/L)	SO_4^{2-} (mg/L)	Cl^- (mg/L)	F^- (mg/L)	Charge Balance Error (%)
LWFDS01	180.072	—	0.685	3.953	-0.014	1.002	0.838	0.054	-3.9
LWFDS05	202.520	—	0.956	3.797	0.005	1.587	1.024	0.098	-2.9
LWFDS07	269.278	—	1.073	3.532	—	3.575	1.150	0.127	-2.9
WFDS08	95.343	0.303	0.404	0.521	0.034	1.421	0.609	0.127	-3.0
WFDS09	333.194	—	1.086	1.661	-0.133	7.688	1.654	0.092	-2.9
WFDS12	214.025	—	1.109	1.385	-0.045	1.705	1.016	0.077	-2.6
WFDS13	315.431	0.309	1.035	1.735	-0.122	22.646	2.686	0.135	-2.5
New Spring #4	226.480	—	1.204	2.608	-0.032	1.880	1.282	0.071	7.2
Five Suns Spring	136.670	0.306	—	2.652	0.011	11.365	2.607	0.072	6.1
W.F. Lower Spring	254.513	—	—	—	—	76.771	1.899	0.099	2.0
FR050 Spring	234.867	—	—	—	—	192.757	2.963	0.084	0.5
W.F. Upper Spring	239.335	—	—	—	—	48.312	1.664	0.084	—
WFDS10	105.737	—	0.351	3.917	0.168	2.028	1.181	0.071	-3.3
WFDS14	282.418	—	1.270	3.281	-0.060	6.393	1.334	0.087	-3.4
WFDS19	240.377	—	1.382	1.779	-0.122	192.358	2.112	0.106	1.2
New Spring #1	187.400	—	0.859	2.492	0.110	11.217	1.620	0.080	0.0
New Spring #2	170.010	—	—	2.451	0.102	11.322	1.656	0.082	5.7
New Spring #3	232.270	—	1.416	1.155	—	143.936	2.347	0.107	4.2
N. Side Spring #1	328.140	—	—	—	—	119.598	6.052	0.074	-23.7
S. Side Spring #1	202.490	0.324	—	1.467	—	53.961	4.178	0.072	-8.5
Upper Spring B	212.180	—	1.170	0.467	—	36.488	1.900	0.090	6.5

Table 6. Field Parameters for West Fork Stream Samples

Temperature, SC, and salinity were recorded during each site visit to the West Fork Gage, and the stream site above the Vat Diversion. These were necessary for the chemical hydrograph separation in order identify any discrepancies between these discrete measurements made using a Multiprobe Hydrolab, and the continuous data from the West Fork Gage, and to estimate the continuous SC at the upstream location.

Site	Sample Date	Sample Time	Temperature (°C)	SC (µS/cm)	Salinity (‰)
West Fork Gage (below Wolf Creek)	3/13/2014	12:30	3.1	531	0.350
	4/17/2014	11:00	4.5	448	0.296
	5/12/2014	13:55	5.3	395	0.261
	5/23/2014	13:47	8.3	343	0.226
	5/27/2014	12:00	12.1	318	0.210
	5/30/2014	9:52	9.9	346	0.228
	6/6/2014	12:45	14.2	359	0.237
	6/19/2014	11:45	11.5	399	0.263
	7/7/2014	10:45	16.4	430	0.284
	9/3/2014	12:35	14.4	473	0.312
	10/9/2014	14:10	11.1	478	0.316
	10/28/2014	—	2.1	515	0.340
	1/5/2015	13:30	0.0	500	0.330
	2/23/2015	11:15	0.1	523	0.345
West Fork above Vat Diversion	5/27/2014	11:00	6.2	238	0.157
	6/6/2014	10:35	6.9	305	0.201
	6/19/2014	10:40	7.0	349	0.230
	7/7/2014	10:00	—	—	0.254
	9/3/2014	13:20	14.0	415	0.274
	10/9/2014	15:35	8.6	420	0.277
	2/23/2015	13:00	0.2	451	0.298

Table 7. Major-ion Chemistry of West Fork Stream Samples

Major cation and anion concentrations were analyzed at the University of Utah using a Metrohm 883 IC Basic Plus ion chromatograph. A Metrohm 905 Titrando titrator was used to measure alkalinity as $CaCO_3$. Charge balance error (%) is defined as $\frac{\sum cations - \sum anions}{\sum cations + \sum anions} \times 100$.

Site	Sample Date	Sample Time	Li^+ (mg/L)	NH^{4+} (mg/L)	Ca^{2+} (mg/L)	Mg^{2+} (mg/L)	Na^+ (mg/L)	K^+ (mg/L)
West Fork Gage (below Wolf Creek)	3/13/2014	12:30	0.002	—	67.252	18.508	5.164	0.853
	4/17/2014	11:00	0.001	0.003	67.925	16.738	5.652	0.943
	5/12/2014	13:55	0.001	—	61.050	14.248	4.564	0.900
	5/23/2014	13:47	0.001	0.005	52.807	11.635	4.156	0.924
	5/27/2014	12:00	0.001	0.003	49.296	10.727	3.835	0.917
	5/30/2014	9:52	0.001	—	53.870	11.863	4.151	0.864
	6/6/2014	12:45	0.002	—	54.906	13.006	4.506	0.854
	6/19/2014	11:45	0.001	0.007	61.474	14.644	4.932	0.839
	7/7/2014	10:45	0.003	—	65.098	16.771	5.772	0.991
	9/3/2014	12:35	0.002	—	69.870	18.847	6.449	0.968
	10/9/2014	14:10	0.002	—	70.498	18.514	6.205	1.032
	10/28/2014	—	0.003	—	34.979	19.209	6.430	1.015
	1/5/2015	13:30	0.004	—	35.501	18.145	6.097	0.936
	2/23/2015	11:15	0.002	0.032	73.308	19.455	5.925	0.881
West Fork above Vat Diversion	5/27/2014	11:00	0.001	0.083	40.052	6.930	2.192	0.841
	6/6/2014	10:35	0.002	—	50.346	9.607	2.887	0.756
	6/19/2014	10:40	0.001	—	57.476	11.891	3.665	0.747
	7/7/2014	10:00	0.003	0.004	54.147	14.589	4.711	0.880
	9/3/2014	13:20	0.003	—	63.472	15.209	5.461	1.022
	10/9/2014	15:35	0.002	—	64.388	14.507	5.163	1.046
	2/23/2015	13:00	0.003	0.004	66.908	14.488	5.719	0.998

Table 7. continued

Site	HCO_3^- (mg/L)	NO_2^- (mg/L)	Br^- (mg/L)	NO_3^- (mg/L)	PO_4^{3-} (mg/L)	SO_4^{2-} (mg/L)	Cl^- (mg/L)	F^- (mg/L)	Charge Balance Error (%)
West Fork Gage (below Wolf Creek)	230.373	—	0.925	0.710	-0.159	67.877	3.296	0.082	-1.71
	223.480	—	0.938	0.107	-0.122	60.315	2.686	0.084	0.29
	235.033	—	0.909	—	-0.145	36.114	2.168	0.080	-2.58
	203.118	0.307	—	0.771	—	29.205	1.845	0.078	-2.83
	188.575	0.310	—	1.021	-0.177	26.512	1.766	0.079	-2.58
	205.375	—	0.835	1.617	—	27.400	1.891	0.082	-2.07
	215.598	—	0.748	0.206	-0.177	29.973	1.980	0.087	-2.38
	239.706	—	1.002	0.075	-0.133	35.447	2.047	0.098	-2.48
	245.976	—	0.897	0.141	-0.106	47.008	2.389	0.103	-1.87
	253.150	—	1.047	—	—	64.069	3.178	0.096	-2.26
	254.297	—	1.095	—	—	65.690	3.309	0.093	-2.81
	264.215	—	—	—	—	70.545	3.362	0.071	-23.77
	221.833	0.314	—	0.845	-0.075	72.097	2.956	0.076	-19.25
	225.102	0.311	—	0.365	-0.091	72.784	3.447	0.089	2.02
West Fork above Vat Diversion	160.942	0.312	—	2.113	-0.120	6.326	1.007	0.068	-2.77
	203.313	—	0.841	1.152	—	10.910	1.159	0.081	-2.50
	233.423	0.304	0.969	0.196	—	17.524	1.210	0.085	-2.80
	244.256	—	1.041	0.379	-0.115	28.881	1.352	0.089	-6.05
	238.425	—	0.992	0.396	0.034	43.407	1.621	0.088	-2.07
	245.476	—	1.213	0.430	-0.034	38.681	1.867	0.092	-2.60
	213.024	0.306	0.245	0.913	-0.038	50.445	1.783	0.089	1.91

Table 8. SF_6, CFCs, and $^3H/^3He$ Data for West Fork Stream Samples

Tritium samples were only collected at several stream site visits during low-flow conditions. Table 3, in the main text, contains the specific ^3H values used for the evaluation of ^3H as a nonvolatile age-dating tracer. SF_6 and CFCs are presented as equivalent air concentrations; values are generally at present-day atmospheric levels confirming that the gas exchange/loss associated with these volatile age-dating methods is too significant to preserve the groundwater signature in the stream.

Site	Sample Date	Sample Time	^3H (TU)	Tritiogenic ^3He (TU)	SF_6 (pptv)	CFC-11 (pptv)	CFC-12 (pptv)	CFC-113 (pptv)
West Fork Gage (below Wolf Creek)	3/13/2014	12:30	–	–	7.74	265.34	533.04	59.73
	4/17/2014	11:00	–	–	8.35	243.98	514.43	61.92
	5/12/2014	13:55	–	–	8.13	216.77	474.48	49.61
	5/27/2014	12:00	–	–	8.37	179.46	416.16	40.91
	6/6/2014	12:45	–	–	9.62	225.70	523.89	54.44
	6/19/2014	11:45	–	–	7.40	198.22	455.43	46.00
	7/7/2014	10:45	–	–	6.97	208.29	495.89	51.33
	9/3/2014	12:35	5.51	6.34E-14	8.63	217.35	510.55	56.92
	10/9/2014	14:10	5.57	6.31E-14	8.22	217.81	499.17	54.89
	1/5/2015	13:30	5.32	5.65E-14	7.35	185.6885	411.6348	44.05602
	2/23/2015	11:15	5.10	3.44E-14	8.06	65.96	386.80	128.58
West Fork above Vat Diversion	6/6/2014	10:35	–	–	8.62	159.07	366.66	36.21
	6/19/2014	10:40	–	–	7.86	194.94	418.68	46.26
	7/7/2014	10:00	–	–	7.71	262.35	587.08	64.60
	9/3/2014	13:20	6.65	7.74E-14	8.16	216.13	507.50	59.31
	10/9/2014	15:35	6.71	7.80E-14	8.02	218.06	490.91	55.14
	2/23/2015	13:00	6.11	4.11E-14	7.60	91.21	354.80	73.35

Table 9. Continuous Stream Data from the West Fork Gage:
March 2014 - March 2015

The West Fork Gage was installed on March 13, 2014 in order to provide a continuous record of stream stage and stream SC for a one year period. This data was used in the chemical hydrograph separation analysis to estimate West Fork baseflow. The gage was programmed to record temperature, SC, and stream stage every 15 minutes. Stage was converted to stream discharge after each data download. The records presented in this table are daily averages of the 15-minute incremental data obtained directly from the gage. Each page provides the averaged data for a given month throughout March 2014 - March 2015.

Date	Temperature (°C)	SC (µS/cm)	Stage (ft)	Discharge (cfs)
3/14/2014	2.44	500	3.47	12.4
3/15/2014	3.05	495	3.48	12.2
3/16/2014	3.08	495	3.45	11.1
3/17/2014	3.36	492	3.47	11.0
3/18/2014	1.15	497	3.49	10.0
3/19/2014	1.71	490	3.47	9.5
3/20/2014	2.18	499	3.48	11.0
3/21/2014	2.70	496	3.47	12.0
3/22/2014	4.19	491	3.45	13.0
3/23/2014	3.17	492	3.46	13.0
3/24/2014	3.46	493	3.46	13.0
3/25/2014	4.21	490	3.47	15.0
3/26/2014	4.06	487	3.48	16.7
3/27/2014	2.84	487	3.48	16.7
3/28/2014	2.58	487	3.47	15.0
3/29/2014	3.93	487	3.46	14.0
3/30/2014	4.18	487	3.48	16.5
3/31/2014	2.17	480	3.48	16.0

Table 9. continued

Date	Temperature (°C)	SC (µS/cm)	Stage (ft)	Discharge (cfs)
4/1/2014	3.07	479	3.49	17.3
4/2/2014	3.51	484	3.48	15.0
4/3/2014	3.56	488	3.46	15.0
4/4/2014	4.20	488	3.47	15.0
4/5/2014	5.40	485	3.47	16.2
4/6/2014	5.12	484	3.47	16.4
4/7/2014	5.47	485	3.48	16.8
4/8/2014	6.70	486	3.50	19.6
4/9/2014	7.25	476	3.57	24.1
4/10/2014	7.02	466	3.63	28.4
4/11/2014	7.20	455	3.67	31.4
4/12/2014	7.19	444	3.72	36.1
4/13/2014	5.75	435	3.75	35.7
4/14/2014	4.45	443	3.66	27.0
4/15/2014	5.81	452	3.64	25.0
4/16/2014	6.35	454	3.63	25.2
4/17/2014	6.66	446	3.64	24.7
4/18/2014	7.81	442	3.70	30.1
4/19/2014	7.21	431	3.75	33.3
4/20/2014	7.75	418	3.80	38.6
4/21/2014	7.35	407	3.84	41.1
4/22/2014	7.95	400	3.86	42.1
4/23/2014	5.98	393	3.87	42.9
4/24/2014	5.37	393	3.86	42.3
4/25/2014	6.84	397	3.86	42.7
4/26/2014	5.51	397	3.89	46.4
4/27/2014	3.60	398	3.90	44.3
4/28/2014	4.44	401	3.88	43.9
4/29/2014	4.21	406	3.87	42.0
4/30/2014	6.05	408	3.85	39.9

Table 9. continued

Date	Temperature (°C)	SC (µS/cm)	Stage (ft)	Discharge (cfs)
5/1/2014	7.04	413	3.81	37.0
5/2/2014	8.61	415	3.80	36.9
5/3/2014	8.97	409	3.84	41.0
5/4/2014	9.46	398	3.86	42.4
5/5/2014	9.52	383	3.87	43.9
5/6/2014	8.09	374	3.89	44.7
5/7/2014	5.54	377	3.89	44.6
5/8/2014	5.89	382	3.89	44.7
5/9/2014	6.22	386	3.89	45.1
5/10/2014	5.85	390	3.88	43.8
5/11/2014	6.09	392	3.87	43.1
5/12/2014	4.79	395	3.87	43.2
5/13/2014	4.02	396	3.87	43.4
5/14/2014	7.54	398	3.87	42.8
5/15/2014	9.13	394	3.86	42.1
5/16/2014	9.57	388	3.85	41.9
5/17/2014	9.69	375	3.87	44.2
5/18/2014	10.38	366	3.90	46.2
5/19/2014	9.56	332	4.07	61.9
5/20/2014	9.72	337	4.00	55.4
5/21/2014	9.00	357	3.90	44.9
5/22/2014	9.02	351	3.91	47.1
5/23/2014	8.38	349	3.94	49.4
5/24/2014	8.47	358	3.96	51.4
5/25/2014	9.75	354	3.89	45.7
5/26/2014	10.98	320	4.06	64.9
5/27/2014	11.73	311	4.07	59.6
5/28/2014	12.17	339	3.90	45.7
5/29/2014	11.57	342	3.90	45.4
5/30/2014	11.36	346	3.90	45.4
5/31/2014	11.03	351	3.89	44.5

Table 9. continued

Date	Temperature (°C)	SC (µS/cm)	Stage (ft)	Discharge (cfs)
6/1/2014	11.28	353	3.88	43.7
6/2/2014	11.51	354	3.87	43.2
6/3/2014	13.23	355	3.87	42.5
6/4/2014	12.44	358	3.86	42.2
6/5/2014	12.16	361	3.86	41.8
6/6/2014	12.29	364	3.86	42.1
6/7/2014	12.08	367	3.86	41.5
6/8/2014	12.47	371	3.85	40.9
6/9/2014	11.84	374	3.84	40.4
6/10/2014	12.69	376	3.84	40.3
6/11/2014	12.61	382	3.84	40.2
6/12/2014	12.63	382	3.84	40.2
6/13/2014	12.99	389	3.83	39.6
6/14/2014	12.70	388	3.83	39.4
6/15/2014	10.90	393	3.83	39.7
6/16/2014	9.52	398	3.84	40.1
6/17/2014	9.14	403	3.84	40.1
6/18/2014	9.09	403	3.84	40.0
6/19/2014	11.04	399	3.83	39.4
6/20/2014	12.32	399	3.82	38.8
6/21/2014	13.60	400	3.82	38.6
6/22/2014	13.16	401	3.82	38.6
6/23/2014	12.98	406	3.82	38.5
6/24/2014	13.34	406	3.82	38.2
6/25/2014	14.41	407	3.81	37.3
6/26/2014	14.08	410	3.80	37.4
6/27/2014	12.87	415	3.82	38.7
6/28/2014	12.75	414	3.82	37.6
6/29/2014	13.87	415	3.79	34.9
6/30/2014	14.77	418	3.76	33.9

Table 9. continued

Date	Temperature (°C)	SC (µS/cm)	Stage (ft)	Discharge (cfs)
7/1/2014	14.09	422	3.75	31.9
7/2/2014	14.87	423	3.73	30.7
7/3/2014	14.82	426	3.72	30.4
7/4/2014	15.15	425	3.73	30.8
7/5/2014	16.43	426	3.69	27.8
7/6/2014	15.88	431	3.68	26.9
7/7/2014	16.80	430	3.67	25.4
7/8/2014	16.95	432	3.64	23.9
7/9/2014	16.82	436	3.64	24.4
7/10/2014	16.26	443	3.66	26.7
7/11/2014	15.82	439	3.71	29.2
7/12/2014	16.37	437	3.68	26.6
7/13/2014	18.01	436	3.65	24.3
7/14/2014	18.21	438	3.63	22.9
7/15/2014	17.93	441	3.62	22.1
7/16/2014	17.60	443	3.60	21.2
7/17/2014	16.58	444	3.60	20.7
7/18/2014	16.68	446	3.59	20.2
7/19/2014	16.60	448	3.59	19.5
7/20/2014	15.56	455	3.57	19.1
7/21/2014	14.94	458	3.59	19.6
7/22/2014	15.99	456	3.56	18.2
7/23/2014	16.05	461	3.55	17.4
7/24/2014	15.83	467	3.55	17.5
7/25/2014	16.15	461	3.55	16.8
7/26/2014	17.06	458	3.54	16.6
7/27/2014	17.23	457	3.53	16.4
7/28/2014	16.32	462	3.54	17.7
7/29/2014	14.64	469	3.60	22.6
7/30/2014	15.07	464	3.64	22.9
7/31/2014	15.98	465	3.58	19.0

Table 9. continued

Date	Temperature (°C)	SC (μS/cm)	Stage (ft)	Discharge (cfs)
8/1/2014	15.78	467	3.57	18.4
8/2/2014	15.19	466	3.56	17.9
8/3/2014	15.70	463	3.56	18.5
8/4/2014	14.50	470	3.59	20.3
8/5/2014	14.38	465	3.60	22.5
8/6/2014	14.39	456	3.65	24.2
8/7/2014	15.37	454	3.61	20.7
8/8/2014	14.77	456	3.58	19.0
8/9/2014	14.71	457	3.57	18.3
8/10/2014	14.37	459	3.55	17.7
8/11/2014	14.05	461	3.57	18.4
8/12/2014	14.34	461	3.56	18.4
8/13/2014	13.87	463	3.57	18.8
8/14/2014	13.88	461	3.58	19.1
8/15/2014	15.34	452	3.57	18.5
8/16/2014	15.21	455	3.54	15.9
8/17/2014	15.22	452	3.51	14.5
8/18/2014	15.01	453	3.50	14.1
8/19/2014	14.55	469	3.51	17.2
8/20/2014	14.07	460	3.61	21.0
8/21/2014	14.02	460	3.60	20.9
8/22/2014	13.28	463	3.57	18.9
8/23/2014	13.41	460	3.67	29.8
8/24/2014	12.00	456	3.69	25.2
8/25/2014	12.81	458	3.65	27.2
8/26/2014	12.88	460	3.68	26.2
8/27/2014	12.20	471	3.65	23.5
8/28/2014	12.47	467	3.65	24.3
8/29/2014	13.44	465	3.60	19.9
8/30/2014	12.92	471	3.56	18.2
8/31/2014	13.65	469	3.55	17.4

Table 9. continued

Date	Temperature (°C)	SC (µS/cm)	Stage (ft)	Discharge (cfs)
9/1/2014	12.58	471	3.54	16.4
9/2/2014	12.92	473	3.52	15.3
9/3/2014	13.53	477	3.51	14.5
9/4/2014	13.81	477	3.50	13.7
9/5/2014	13.31	481	3.50	14.5
9/6/2014	12.94	484	3.51	14.4
9/7/2014	13.08	485	3.51	14.8
9/8/2014	13.45	483	3.53	17.6
9/9/2014	12.67	479	3.68	31.8
9/10/2014	11.43	463	3.72	26.9
9/11/2014	11.42	462	3.62	21.4
9/12/2014	10.79	465	3.58	19.5
9/13/2014	10.54	468	3.57	18.7
9/14/2014	11.13	469	3.56	17.7
9/15/2014	11.43	471	3.55	17.2
9/16/2014	11.48	473	3.54	16.9
9/17/2014	12.12	473	3.54	16.6
9/18/2014	12.16	473	3.53	16.3
9/19/2014	12.88	472	3.53	15.9
9/20/2014	12.56	472	3.52	15.3
9/21/2014	11.81	476	3.54	19.0
9/22/2014	11.40	473	3.65	24.6
9/23/2014	12.23	472	3.60	20.0
9/24/2014	12.21	472	3.57	18.3
9/25/2014	12.58	477	3.54	16.5
9/26/2014	12.48	478	3.53	16.3
9/27/2014	11.78	484	3.56	25.5
9/28/2014	9.94	439	4.07	65.1
9/29/2014	9.39	441	3.90	41.8
9/30/2014	9.27	458	3.72	27.3

Table 9. continued

Date	Temperature (°C)	SC (µS/cm)	Stage (ft)	Discharge (cfs)
10/1/2014	8.47	472	3.67	25.6
10/2/2014	7.15	475	3.65	24.4
10/3/2014	7.71	486	3.63	23.0
10/4/2014	8.18	494	3.63	22.6
10/5/2014	8.59	491	3.62	22.3
10/6/2014	9.06	496	3.61	20.9
10/7/2014	9.00	502	3.55	17.3
10/8/2014	9.22	490	3.56	18.8
10/9/2014	8.91	482	3.57	19.0
10/10/2014	8.17	484	3.57	19.0
10/11/2014	8.24	482	3.58	19.2
10/12/2014	7.36	479	3.60	21.0
10/13/2014	5.94	482	3.59	19.6
10/14/2014	6.31	484	3.57	19.0
10/15/2014	6.85	483	3.57	18.9
10/16/2014	6.95	491	3.57	18.6
10/17/2014	6.65	498	3.57	18.4
10/18/2014	7.20	495	3.56	18.3
10/19/2014	6.81	502	3.56	17.7
10/20/2014	6.82	496	3.55	17.0
10/21/2014	7.29	495	3.55	17.4
10/22/2014	6.13	494	3.55	16.7
10/23/2014	5.58	489	3.53	16.4
10/24/2014	5.92	490	3.54	16.5
10/25/2014	5.92	490	3.54	16.7
10/26/2014	6.71	488	3.54	16.9
10/27/2014	4.53	491	3.54	16.5
10/28/2014	3.44	494	3.53	15.7
10/29/2014	3.36	498	3.51	14.8
10/30/2014	4.17	496	3.50	14.2
10/31/2014	4.33	494	3.50	15.1

Table 9. continued

Date	Temperature (°C)	SC (µS/cm)	Stage (ft)	Discharge (cfs)
11/1/2014	4.76	490	3.57	19.6
11/2/2014	4.96	485	3.57	18.5
11/3/2014	3.48	487	3.55	17.0
11/4/2014	1.57	493	3.52	12.0
11/5/2014	2.93	495	3.49	13.6
11/6/2014	3.17	489	3.50	14.3
11/7/2014	3.54	486	3.49	13.6
11/8/2014	3.20	488	3.50	13.9
11/9/2014	3.19	487	3.50	14.2
11/10/2014	3.14	486	3.52	13.0
11/11/2014	0.85	478	3.58	11.0
11/12/2014	0.30	488	3.56	10.0
11/13/2014	-0.01	494	3.73	9.0
11/14/2014	0.18	492	3.92	10.0
11/15/2014	0.81	487	3.52	13.0
11/16/2014	0.02	472	3.70	12.0
11/17/2014	-0.01	492	3.90	12.0
11/18/2014	0.01	478	3.75	14.0
11/19/2014	0.03	500	3.76	16.0
11/20/2014	0.45	489	3.58	18.0
11/21/2014	0.32	488	3.64	17.0
11/22/2014	0.25	484	3.62	17.0
11/23/2014	0.31	490	3.57	18.9
11/24/2014	0.10	485	3.64	17.0
11/25/2014	0.11	479	3.71	16.0
11/26/2014	0.96	484	3.55	16.6
11/27/2014	0.38	481	3.60	16.0
11/28/2014	0.65	476	3.56	15.0
11/29/2014	0.55	488	3.58	15.0
11/30/2014	1.74	481	3.53	16.0

Table 9. continued

Date	Temperature (°C)	SC (µS/cm)	Stage (ft)	Discharge (cfs)
12/1/2014	1.47	483	3.52	15.0
12/2/2014	0.57	490	3.58	15.0
12/3/2014	1.55	488	3.54	15.9
12/4/2014	2.60	483	3.53	16.1
12/5/2014	1.24	489	3.53	15.0
12/6/2014	1.98	487	3.52	15.6
12/7/2014	1.16	492	3.52	14.0
12/8/2014	0.61	496	3.51	14.0
12/9/2014	0.26	496	3.63	13.0
12/10/2014	0.16	482	3.62	13.0
12/11/2014	0.14	490	3.64	12.0
12/12/2014	0.91	496	3.53	14.0
12/13/2014	1.97	487	3.50	14.1
12/14/2014	0.69	490	3.52	14.0
12/15/2014	-0.01	506	3.72	13.0
12/16/2014	-0.01	511	3.97	14.0
12/17/2014	0.09	478	3.62	14.0
12/18/2014	0.04	485	3.70	14.0
12/19/2014	-0.01	509	3.68	13.0
12/20/2014	0.20	499	3.66	14.0
12/21/2014	0.45	493	3.51	14.5
12/22/2014	0.55	471	3.56	14.0
12/23/2014	0.01	495	3.60	13.0
12/24/2014	-0.01	511	3.96	13.0
12/25/2014	-0.01	499	4.15	14.0
12/26/2014	-0.01	504	4.27	13.0
12/27/2014	-0.01	523	4.46	12.0
12/28/2014	-0.01	516	4.57	13.0
12/29/2014	-0.01	505	4.55	13.0
12/30/2014	-0.01	505	4.53	12.0
12/31/2014	-0.01	522	4.50	10.0

Table 9. continued

Date	Temperature (°C)	SC (µS/cm)	Stage (ft)	Discharge (cfs)
1/1/2015	-0.01	530	4.52	11.0
1/2/2015	-0.01	518	4.48	12.0
1/3/2015	-0.01	507	4.16	14.0
1/4/2015	-0.01	497	4.18	13.0
1/5/2015	-0.01	494	4.21	15.0
1/6/2015	0.01	490	3.87	16.0
1/7/2015	0.03	496	3.69	15.0
1/8/2015	0.08	501	3.69	16.0
1/9/2015	0.09	502	3.58	15.0
1/10/2015	0.21	502	3.54	16.0
1/11/2015	0.77	495	3.50	14.1
1/12/2015	0.76	489	3.50	14.1
1/13/2015	0.62	489	3.50	14.0
1/14/2015	0.09	501	3.59	13.0
1/15/2015	-0.01	512	4.06	14.0
1/16/2015	-0.01	513	4.07	13.0
1/17/2015	0.01	503	3.83	12.0
1/18/2015	0.06	504	3.81	12.0
1/19/2015	0.35	502	3.55	13.0
1/20/2015	0.33	498	3.51	14.0
1/21/2015	0.01	510	3.65	12.0
1/22/2015	-0.01	531	4.02	11.0
1/23/2015	-0.01	514	4.07	13.0
1/24/2015	0.00	514	3.66	12.0
1/25/2015	0.15	501	3.53	12.0
1/26/2015	0.46	497	3.50	13.0
1/27/2015	0.44	499	3.52	14.0
1/28/2015	1.01	490	3.50	13.9
1/29/2015	0.50	493	3.51	14.0
1/30/2015	1.04	489	3.49	13.6
1/31/2015	1.07	487	3.50	13.6

Table 9. continued

Date	Temperature (°C)	SC (µS/cm)	Stage (ft)	Discharge (cfs)
2/1/2015	0.17	497	3.53	14.0
2/2/2015	0.84	496	3.50	14.1
2/3/2015	1.59	489	3.49	13.4
2/4/2015	2.21	483	3.50	14.5
2/5/2015	1.29	486	3.50	14.3
2/6/2015	1.17	493	3.50	14.4
2/7/2015	1.62	494	3.50	14.1
2/8/2015	2.18	491	3.50	14.5
2/9/2015	1.92	492	3.50	14.4
2/10/2015	2.14	496	3.51	14.9
2/11/2015	1.11	499	3.51	15.0
2/12/2015	1.22	500	3.50	14.4
2/13/2015	1.65	498	3.48	13.1
2/14/2015	1.96	497	3.49	13.5
2/15/2015	2.42	494	3.50	14.3
2/16/2015	2.08	492	3.51	14.9
2/17/2015	0.71	504	3.52	14.0
2/18/2015	0.51	505	3.57	13.0
2/19/2015	1.40	498	3.52	15.0
2/20/2015	1.73	495	3.51	14.0
2/21/2015	1.46	494	3.50	13.0
2/22/2015	0.80	499	3.49	13.0
2/23/2015	0.42	506	3.56	13.0
2/24/2015	0.21	496	3.60	11.0
2/25/2015	0.79	502	3.52	12.0
2/26/2015	1.11	484	3.51	13.0
2/27/2015	0.48	490	3.53	12.0
2/28/2015	0.58	501	3.51	12.0

Table 9. continued

Date	Temperature (°C)	SC (µS/cm)	Stage (ft)	Discharge (cfs)
3/1/2015	1.28	496	3.48	12.7
3/2/2015	1.53	492	3.48	13.2
3/3/2015	1.31	482	3.49	13.0
3/4/2015	0.41	504	3.55	13.0
3/5/2015	0.28	508	3.60	12.0
3/6/2015	0.82	500	3.53	12.0
3/7/2015	1.86	500	3.50	13.0
3/8/2015	2.51	492	3.50	13.0
3/9/2015	2.58	495	3.50	13.0
3/10/2015	3.00	487	3.49	13.0
3/11/2015	2.81	487	3.49	13.2
3/12/2015	3.92	484	3.49	14.4
3/13/2015	4.24	477	3.53	15.9

Table 10. Vat Diversion Records: March 2014 - March 2015

The following pages contain daily Vat Diversion records provided by the Central Utah Water Conservancy District (CUWCD) for March 2014 through March 2015. The column labeled, *Releases*, gives the volume of water (per second) that is allowed to flow past the diversion structure and return into the main channel of the West Fork. *Diversions* signifies the rate at which water is being taken from the West Fork and transported into Currant Creek Reservoir via the West Fork Pipeline. *Inflow* is a measure of the water flowing down the West Fork above the Diversion Dam.

Date	Reservoir Elevation (ft)	Total Storage (AF)	Change in Reservoir (AF)	Releases (cfs)	Diversions (cfs)	Inflow (cfs)
01-Mar-14	7,810.77	35	0	6	0	6
02-Mar-14	7,810.63	34	-1	6	0	5
03-Mar-14	7,810.47	33	-1	6	0	5
04-Mar-14	7,810.32	32	-1	6	0	5
05-Mar-14	7,810.17	31	-1	6	0	5
06-Mar-14	7,810.04	31	0	6	0	6
07-Mar-14	7,810.02	31	0	6	0	6
08-Mar-14	7,809.89	30	-1	6	0	5
09-Mar-14	7,809.73	29	-1	6	0	5
10-Mar-14	7,809.94	30	1	6	0	7
11-Mar-14	7,810.09	31	1	6	0	7
12-Mar-14	7,809.85	30	-1	6	0	5
13-Mar-14	7,809.91	30	0	6	0	6
14-Mar-14	7,809.93	30	0	6	0	6
15-Mar-14	7,810.12	31	1	6	0	7
16-Mar-14	7,810.15	31	0	6	0	6
17-Mar-14	7,810.35	33	2	6	0	7
18-Mar-14	7,810.17	31	-2	6	0	5
19-Mar-14	7,809.99	30	-1	6	0	5
20-Mar-14	7,809.93	30	0	6	0	6
21-Mar-14	7,810.06	31	1	6	0	7
22-Mar-14	7,810.24	32	1	6	0	7
23-Mar-14	7,810.08	31	-1	6	0	5
24-Mar-14	7,810.22	32	1	6	0	7
25-Mar-14	7,810.45	33	1	6	0	7
26-Mar-14	7,810.90	36	3	6	0	8
27-Mar-14	7,810.97	36	0	6	0	6
28-Mar-14	7,810.91	36	0	6	0	6
29-Mar-14	7,810.90	36	0	6	0	6
30-Mar-14	7,810.97	36	0	6	0	6
31-Mar-14	7,810.90	36	0	6	0	6

	Releases	Diversions	Inflow
AVERAGE IN CFS	6	0	6
TOTALS IN ACRE FEET	369	0	369

Table 10. continued

Date	Reservoir Elevation (ft)	Total Storage (AF)	Change in Reservoir (AF)	Releases (cfs)	Diversions (cfs)	Inflow (cfs)
01-Apr-14	7,810.98	36	0	6	0	6
02-Apr-14	7,810.88	36	0	6	0	6
03-Apr-14	7,810.86	36	0	6	0	6
04-Apr-14	7,810.86	36	0	6	0	6
05-Apr-14	7,810.96	36	0	6	0	6
06-Apr-14	7,810.96	36	0	6	0	6
07-Apr-14	7,810.96	36	0	6	0	6
08-Apr-14	7,810.90	36	0	7	0	7
09-Apr-14	7,810.77	35	-1	10	0	9
10-Apr-14	7,810.82	35	0	13	0	13
11-Apr-14	7,810.90	36	1	15	0	16
12-Apr-14	7,810.88	36	0	18	0	18
13-Apr-14	7,810.39	33	-3	17	0	15
14-Apr-14	7,810.33	32	-1	14	0	13
15-Apr-14	7,810.32	32	0	13	0	13
16-Apr-14	7,810.34	32	0	14	0	14
17-Apr-14	7,810.36	33	1	15	0	16
18-Apr-14	7,810.42	33	0	19	0	19
19-Apr-14	7,810.46	33	0	21	0	21
20-Apr-14	7,810.51	33	0	23	0	23
21-Apr-14	7,810.42	33	0	25	4	29
22-Apr-14	7,810.18	31	-2	25	10	34
23-Apr-14	7,810.22	32	1	25	14	40
24-Apr-14	7,810.06	31	-1	25	4	28
25-Apr-14	7,810.16	31	0	25	9	34
26-Apr-14	7,810.18	31	0	25	12	37
27-Apr-14	7,809.98	30	-1	25	2	26
28-Apr-14	7,809.79	29	-1	25	0	24
29-Apr-14	7,808.55	23	-6	24	0	21
30-Apr-14	7,807.37	17	-6	22	0	19

	Releases	Diversions	Inflow
AVERAGE IN CFS	16	2	18
TOTALS IN ACRE FEET	966	109	1,053

Table 10. continued

Date	Reservoir Elevation (ft)	Total Storage (AF)	Change in Reservoir (AF)	Releases (cfs)	Diversions (cfs)	Inflow (cfs)
01-May-14	7,807.78	29	17	21	0	30
02-May-14	7,809.33	27	-2	22	3	24
03-May-14	7,809.79	29	2	24	17	42
04-May-14	7,810.20	32	3	24	44	70
05-May-14	7,810.28	32	0	24	73	97
06-May-14	7,810.07	31	-1	23	76	98
07-May-14	7,809.69	29	-2	24	44	67
08-May-14	7,809.71	29	0	24	34	58
09-May-14	7,809.63	28	-1	25	29	53
10-May-14	7,809.60	28	0	24	26	50
11-May-14	7,809.56	28	0	24	23	47
12-May-14	7,809.63	28	0	24	19	43
13-May-14	7,809.70	29	1	25	15	41
14-May-14	7,809.81	29	0	25	18	43
15-May-14	7,810.02	31	2	25	36	62
16-May-14	7,810.10	31	0	25	68	93
17-May-14	7,810.52	34	3	27	104	133
18-May-14	7,810.14	31	-3	38	132	168
19-May-14	7,810.87	36	5	48	148	199
20-May-14	7,810.43	33	-3	30	166	194
21-May-14	7,809.85	30	-3	26	163	187
22-May-14	7,810.08	31	1	31	171	203
23-May-14	7,810.14	31	0	27	165	192
24-May-14	7,809.54	28	-3	31	154	183
25-May-14	7,807.95	20	-8	39	170	205
26-May-14	7,811.22	38	18	52	193	254
27-May-14	7,810.01	30	-8	31	208	235
28-May-14	7,808.96	25	-5	25	188	210
29-May-14	7,808.94	25	0	25	165	190
30-May-14	7,808.94	25	0	25	141	166
31-May-14	7,808.96	25	0	24	123	147

	Releases	Diversions	Inflow
AVERAGE IN CFS	28	94	122
TOTALS IN ACRE FEET	1,710	5,784	7,505

Table 10. continued

Date	Reservoir Elevation (ft)	Total Storage (AF)	Change in Reservoir (AF)	Releases (cfs)	Diversions (cfs)	Inflow (cfs)
01-Jun-14	7,808.99	25	0	24	106	130
02-Jun-14	7,808.98	25	0	24	94	118
03-Jun-14	7,808.98	25	0	24	86	110
04-Jun-14	7,808.97	25	0	24	77	101
05-Jun-14	7,808.97	25	0	24	73	97
06-Jun-14	7,808.92	25	0	24	59	83
07-Jun-14	7,809.05	25	0	24	42	66
08-Jun-14	7,809.13	26	1	24	33	58
09-Jun-14	7,809.80	29	3	24	35	61
10-Jun-14	7,808.79	24	-5	24	32	53
11-Jun-14	7,808.98	25	1	25	26	52
12-Jun-14	7,809.31	27	2	24	23	48
13-Jun-14	7,809.44	27	0	24	21	45
14-Jun-14	7,809.43	27	0	24	18	42
15-Jun-14	7,809.47	28	1	24	16	41
16-Jun-14	7,809.49	28	0	24	14	38
17-Jun-14	7,809.47	28	0	24	14	38
18-Jun-14	7,809.50	28	0	24	14	38
19-Jun-14	7,809.43	27	-1	24	10	33
20-Jun-14	7,809.45	27	0	24	5	29
21-Jun-14	7,809.43	27	0	24	2	26
22-Jun-14	7,809.44	27	0	24	1	25
23-Jun-14	7,809.41	27	0	24	0	24
24-Jun-14	7,809.33	27	0	24	0	24
25-Jun-14	7,808.90	24	-3	23	0	21
26-Jun-14	7,808.19	21	-3	23	0	21
27-Jun-14	7,807.25	17	-4	24	0	22
28-Jun-14	7,806.19	13	-4	24	0	22
29-Jun-14	7,804.89	9	-4	23	0	21
30-Jun-14	7,803.54	5	-4	23	0	21

	Releases	Diversions	Inflow
AVERAGE IN CFS	24	27	50
TOTALS IN ACRE FEET	1,422	1,589	2,991

Table 10. continued

Date	Reservoir Elevation (ft)	Total Storage (AF)	Change in Reservoir (AF)	Releases (cfs)	Diversions (cfs)	Inflow (cfs)
01-Jul-14	7,802.95	4	-1	20	0	19
02-Jul-14	7,802.94	4	0	20	0	20
03-Jul-14	7,802.94	4	0	20	0	20
04-Jul-14	7,802.94	4	0	20	0	20
05-Jul-14	7,802.95	4	0	20	0	20
06-Jul-14	7,802.94	4	0	20	0	20
07-Jul-14	7,802.95	4	0	18	0	18
08-Jul-14	7,802.94	4	0	18	0	18
09-Jul-14	7,802.93	4	0	18	0	18
10-Jul-14	7,802.92	4	0	18	0	18
11-Jul-14	7,802.93	4	0	18	0	18
12-Jul-14	7,802.92	4	0	18	0	18
13-Jul-14	7,802.92	4	0	18	0	18
14-Jul-14	7,802.93	4	0	18	0	18
15-Jul-14	7,802.93	4	0	18	0	18
16-Jul-14	7,802.93	4	0	18	0	18
17-Jul-14	7,802.94	4	0	18	0	18
18-Jul-14	7,802.95	4	0	17	0	17
19-Jul-14	7,802.95	4	0	17	0	17
20-Jul-14	7,802.94	4	0	17	0	17
21-Jul-14	7,802.94	4	0	17	0	17
22-Jul-14	7,802.96	4	0	16	0	16
23-Jul-14	7,802.94	4	0	16	0	16
24-Jul-14	7,802.93	4	0	16	0	16
25-Jul-14	7,802.94	4	0	16	0	16
26-Jul-14	7,802.93	4	0	16	0	16
27-Jul-14	7,802.93	4	0	16	0	16
28-Jul-14	7,802.92	4	0	14	0	14
29-Jul-14	7,803.17	4	0	11	0	11
30-Jul-14	7,804.97	9	5	12	0	15
31-Jul-14	7,807.31	17	8	11	0	15

	Releases	Diversions	Inflow
AVERAGE IN CFS	17	0	17
TOTALS IN ACRE FEET	1,051	0	1,063

Table 10. continued

Date	Reservoir Elevation (ft)	Total Storage (AF)	Change in Reservoir (AF)	Releases (cfs)	Diversions (cfs)	Inflow (cfs)
01-Aug-14	7,808.58	23	6	10	0	13
02-Aug-14	7,809.44	27	4	10	0	12
03-Aug-14	7,809.82	29	2	11	0	12
04-Aug-14	7,810.47	33	4	10	0	12
05-Aug-14	7,811.17	38	5	16	0	19
06-Aug-14	7,811.20	38	0	15	0	15
07-Aug-14	7,811.18	38	0	13	0	13
08-Aug-14	7,811.17	38	0	12	0	12
09-Aug-14	7,811.17	38	0	12	0	12
10-Aug-14	7,811.18	38	0	13	0	13
11-Aug-14	7,811.19	38	0	14	0	14
12-Aug-14	7,811.19	38	0	14	0	14
13-Aug-14	7,811.19	38	0	14	0	14
14-Aug-14	7,811.20	38	0	15	0	15
15-Aug-14	7,811.19	38	0	14	0	14
16-Aug-14	7,811.17	38	0	12	0	12
17-Aug-14	7,811.16	38	0	11	0	11
18-Aug-14	7,811.15	37	-1	10	0	9
19-Aug-14	7,811.17	38	1	12	0	13
20-Aug-14	7,811.19	38	0	15	0	15
21-Aug-14	7,811.20	38	0	15	0	15
22-Aug-14	7,811.19	38	0	14	0	14
23-Aug-14	7,811.28	38	0	25	0	25
24-Aug-14	7,811.21	38	0	16	0	16
25-Aug-14	7,811.23	38	0	19	0	19
26-Aug-14	7,811.20	38	0	16	0	16
27-Aug-14	7,811.20	38	0	15	0	15
28-Aug-14	7,811.21	38	0	17	0	17
29-Aug-14	7,811.19	38	0	13	0	13
30-Aug-14	7,811.18	38	0	13	0	13
31-Aug-14	7,811.17	38	0	12	0	12

	Releases	Diversions	Inflow
AVERAGE IN CFS	14	0	14
TOTALS IN ACRE FEET	849	0	871

Table 10. continued

Date	Reservoir Elevation (ft)	Total Storage (AF)	Change in Reservoir (AF)	Releases (cfs)	Diversions (cfs)	Inflow (cfs)
01-Sep-14	7,811.16	38	0	11	0	11
02-Sep-14	7,811.16	38	0	10	0	10
03-Sep-14	7,811.15	37	-1	10	0	9
04-Sep-14	7,811.14	37	0	9	0	9
05-Sep-14	7,811.15	37	0	10	0	10
06-Sep-14	7,811.16	38	1	10	0	11
07-Sep-14	7,811.15	37	-1	10	0	9
08-Sep-14	7,811.17	38	1	12	0	13
09-Sep-14	7,811.27	38	0	24	0	24
10-Sep-14	7,811.21	38	0	16	0	16
11-Sep-14	7,811.18	38	0	13	0	13
12-Sep-14	7,811.17	38	0	12	0	12
13-Sep-14	7,811.16	38	0	12	0	12
14-Sep-14	7,811.16	38	0	11	0	11
15-Sep-14	7,811.16	38	0	10	0	10
16-Sep-14	7,811.15	37	-1	10	0	9
17-Sep-14	7,811.15	37	0	10	0	10
18-Sep-14	7,811.15	37	0	10	0	10
19-Sep-14	7,811.15	37	0	10	0	10
20-Sep-14	7,811.14	37	0	9	0	9
21-Sep-14	7,811.19	38	1	14	0	15
22-Sep-14	7,811.21	38	0	16	0	16
23-Sep-14	7,811.18	38	0	13	0	13
24-Sep-14	7,811.16	38	0	12	0	12
25-Sep-14	7,811.16	38	0	11	0	11
26-Sep-14	7,811.15	37	-1	10	0	9
27-Sep-14	7,811.26	38	1	23	0	24
28-Sep-14	7,811.44	39	1	50	0	51
29-Sep-14	7,811.07	37	-2	25	4	28
30-Sep-13	7,810.12	31	-6	12	0	9

	Releases	Diversions	Inflow
AVERAGE IN CFS	14	0	14
TOTALS IN ACRE FEET	823	8	825

Table 10. continued

Date	Reservoir Elevation (ft)	Total Storage (AF)	Change in Reservoir (AF)	Releases (cfs)	Diversions (cfs)	Inflow (cfs)
01-Oct-14	7,810.43	33	2	13	1	15
02-Oct-14	7,810.43	33	0	13	1	14
03-Oct-14	7,810.43	33	0	13	0	13
04-Oct-14	7,810.31	32	-1	13	0	12
05-Oct-14	7,810.00	25	-7	13	0	9
06-Oct-14	7,809.89	30	5	10	0	13
07-Oct-14	7,810.57	34	4	10	0	12
08-Oct-14	7,810.67	34	0	11	0	11
09-Oct-14	7,810.51	33	-1	11	0	10
10-Oct-14	7,810.29	32	-1	11	0	10
11-Oct-14	7,810.04	31	-1	11	0	10
12-Oct-14	7,809.98	30	-1	11	0	10
13-Oct-14	7,810.09	31	1	10	0	11
14-Oct-14	7,810.06	31	0	10	0	10
15-Oct-14	7,810.00	30	-1	10	0	9
16-Oct-14	7,809.87	30	0	10	0	10
17-Oct-14	7,809.67	29	-1	10	0	9
18-Oct-14	7,809.46	27	-2	10	0	9
19-Oct-14	7,809.37	27	0	9	0	9
20-Oct-14	7,809.41	27	0	9	0	9
21-Oct-14	7,809.48	28	1	9	0	10
22-Oct-14	7,809.52	28	0	9	0	9
23-Oct-14	7,809.47	28	0	9	0	9
24-Oct-14	7,809.46	27	-1	8	0	7
25-Oct-14	7,809.40	27	0	8	0	8
26-Oct-14	7,809.39	27	0	8	0	8
27-Oct-14	7,809.39	27	0	8	0	8
28-Oct-14	7,809.32	27	0	8	0	8
29-Oct-14	7,809.34	27	0	7	0	7
30-Oct-14	7,809.69	29	2	7	0	8
31-Oct-14	7,809.58	28	-1	9	0	8

	Releases	Diversions	Inflow
AVERAGE IN CFS	10	0	10
TOTALS IN ACRE FEET	611	4	605

Table 10. continued

Date	Reservoir Elevation (ft)	Total Storage (AF)	Change in Reservoir (AF)	Releases (cfs)	Diversions (cfs)	Inflow (cfs)
01-Nov-14	7,808.22	21	-7	10	0	6
02-Nov-14	7,807.03	16	-5	10	0	7
03-Nov-14	7,806.20	13	-3	8	0	6
04-Nov-14	7,805.77	12	-1	6	0	5
05-Nov-14	7,807.07	16	4	6	0	8
06-Nov-14	7,808.25	21	5	5	0	8
07-Nov-14	7,809.41	27	6	5	0	8
08-Nov-14	7,810.21	32	5	5	0	8
09-Nov-14	7,810.79	35	3	6	0	8
10-Nov-14	7,810.97	36	1	7	0	8
11-Nov-14	7,810.12	31	-5	7	0	4
12-Nov-14	7,809.42	27	-4	7	0	5
13-Nov-14	7,809.11	26	-1	6	0	5
14-Nov-14	7,809.86	30	4	5	0	7
15-Nov-14	7,810.83	35	5	6	0	9
16-Nov-14	7,811.11	37	2	6	0	7
17-Nov-14	7,811.23	38	1	6	0	7
18-Nov-14	7,810.80	35	-3	7	0	5
19-Nov-14	7,810.53	34	-1	7	0	6
20-Nov-14	7,810.33	32	-2	7	0	6
21-Nov-14	7,810.10	31	-1	7	0	6
22-Nov-14	7,809.91	30	-1	7	0	6
23-Nov-14	7,809.89	30	0	7	0	7
24-Nov-14	7,809.90	30	0	7	0	7
25-Nov-14	7,810.10	31	1	7	0	8
26-Nov-14	7,810.38	33	2	7	0	8
27-Nov-14	7,810.54	34	1	7	0	8
28-Nov-14	7,810.67	34	0	7	0	7
29-Nov-14	7,810.75	35	1	7	0	8
30-Nov-14	7,810.79	35	0	7	0	7

	Releases	Diversions	Inflow
AVERAGE IN CFS	7	0	7
TOTALS IN ACRE FEET	401	0	407

Table 10. continued

Date	Reservoir Elevation (ft)	Total Storage (AF)	Change in Reservoir (AF)	Releases (cfs)	Diversions (cfs)	Inflow (cfs)
01-Dec-14	7,810.81	35	1	7	0	8
02-Dec-14	7,810.68	34	-1	7	0	6
03-Dec-14	7,810.76	35	1	7	0	8
04-Dec-14	7,810.82	35	0	7	0	7
05-Dec-14	7,810.84	35	0	8	0	8
06-Dec-14	7,810.81	35	0	7	0	7
07-Dec-14	7,810.68	34	-1	7	0	6
08-Dec-14	7,810.46	33	-1	8	0	7
09-Dec-14	7,810.24	32	-1	8	0	7
10-Dec-14	7,810.23	32	0	7	0	7
11-Dec-14	7,810.12	31	-1	7	0	6
12-Dec-14	7,810.30	32	1	7	0	8
13-Dec-14	7,810.34	32	0	7	0	7
14-Dec-14	7,810.35	33	1	7	0	8
15-Dec-14	7,809.99	30	-3	7	0	5
16-Dec-14	7,809.98	30	0	7	0	7
17-Dec-14	7,810.09	31	1	7	0	8
18-Dec-14	7,810.01	30	-1	7	0	6
19-Dec-14	7,809.81	29	-1	7	0	6
20-Dec-14	7,809.88	30	1	7	0	8
21-Dec-14	7,809.91	30	0	7	0	7
22-Dec-14	7,810.03	31	1	7	0	8
23-Dec-14	7,809.73	29	-2	7	0	6
24-Dec-14	7,809.88	30	1	7	0	8
25-Dec-14	7,810.27	32	2	7	0	8
26-Dec-14	7,810.37	33	1	7	0	8
27-Dec-14	7,810.22	32	-1	7	0	6
28-Dec-14	7,810.20	32	0	7	0	7
29-Dec-14	7,810.19	32	0	7	0	7
30-Dec-14	7,810.14	31	-1	7	0	6
31-Dec-14	7,809.87	30	-1	7	0	6

	Releases (cfs)	Diversions (cfs)	Inflow (cfs)
AVERAGE IN CFS	7	0	7
TOTALS IN ACRE FEET	436	0	430

Table 10. continued

Date	Reservoir Elevation (ft)	Total Storage (AF)	Change in Reservoir (AF)	Releases (cfs)	Diversions (cfs)	Inflow (cfs)
01-Jan-15	7,809.80	29	0	7	0	7
02-Jan-15	7,809.74	29	0	7	0	7
03-Jan-15	7,809.68	29	0	7	0	7
04-Jan-15	7,809.59	28	-1	7	0	6
05-Jan-15	7,809.51	28	0	7	0	7
06-Jan-15	7,809.45	27	-1	7	0	6
07-Jan-15	7,809.40	27	0	7	0	7
08-Jan-15	7,809.33	27	0	7	0	7
09-Jan-15	7,809.21	26	-1	7	0	6
10-Jan-15	7,809.23	26	0	7	0	7
11-Jan-15	7,809.26	26	0	7	0	7
12-Jan-15	7,809.28	26	0	7	0	7
13-Jan-15	7,809.34	27	1	7	0	8
14-Jan-15	7,808.88	24	-3	7	0	5
15-Jan-15	7,808.96	25	1	6	0	7
16-Jan-15	7,809.89	30	5	6	0	9
17-Jan-15	7,810.57	34	4	6	0	8
18-Jan-15	7,811.00	30	-4	9	0	7
19-Jan-15	7,810.97	30	0	8	0	8
20-Jan-15	7,810.97	30	0	7	0	7
21-Jan-15	7,810.26	32	2	8	0	9
22-Jan-15	7,809.91	30	-2	7	0	6
23-Jan-15	7,810.18	31	1	6	0	7
24-Jan-15	7,810.20	32	1	6	0	7
25-Jan-15	7,810.20	32	0	6	0	6
26-Jan-15	7,810.53	34	2	7	0	8
27-Jan-15	7,810.34	32	-2	7	0	6
28-Jan-15	7,810.17	31	-1	7	0	6
29-Jan-15	7,809.95	30	-1	7	0	6
30-Jan-15	7,809.80	29	-1	7	0	6
31-Jan-15	7,809.71	29	0	7	0	7

	Releases	Diversions	Inflow
AVERAGE IN CFS	7	0	7
TOTALS IN ACRE FEET	426	0	424

Table 10. continued

Date	Reservoir Elevation (ft)	Total Storage (AF)	Change in Reservoir (AF)	Releases (cfs)	Diversions (cfs)	Inflow (cfs)
01-Feb-15	7,809.39	27	0	7	0	7
02-Feb-15	7,809.40	27	0	7	0	7
03-Feb-15	7,809.32	27	0	7	0	7
04-Feb-15	7,809.31	27	0	7	0	7
05-Feb-15	7,809.26	26	-1	7	0	6
06-Feb-15	7,809.00	25	-1	7	0	6
07-Feb-15	7,809.12	26	1	7	0	8
08-Feb-15	7,809.26	26	0	7	0	7
09-Feb-15	7,809.31	27	1	7	0	8
10-Feb-15	7,809.53	28	1	7	0	8
11-Feb-15	7,809.20	26	-2	6	0	5
12-Feb-15	7,809.58	28	2	6	0	7
13-Feb-15	7,810.24	32	4	6	0	8
14-Feb-15	7,810.75	35	3	6	0	8
15-Feb-15	7,810.87	36	1	7	0	8
16-Feb-15	7,810.59	34	-2	8	0	7
17-Feb-15	7,809.62	28	-6	7	0	4
18-Feb-15	7,809.65	28	0	7	0	7
19-Feb-15	7,809.86	30	2	7	0	8
20-Feb-15	7,809.91	30	0	7	0	7
21-Feb-15	7,809.75	29	-1	7	0	6
22-Feb-15	7,809.35	27	-2	7	0	6
23-Feb-15	7,809.08	25	-2	7	0	6
24-Feb-15	7,808.64	23	-2	7	0	6
25-Feb-15	7,809.14	26	3	7	0	9
26-Feb-15	7,809.04	25	-1	7	0	6
27-Feb-15	7,809.02	25	0	7	0	7
28-Feb-15	7,809.09	25	0	7	0	7

	Releases (cfs)	Diversions (cfs)	Inflow (cfs)
AVERAGE IN CFS	7	0	7
TOTALS IN ACRE FEET	383	0	383

Table 10. continued

Date	Reservoir Elevation (ft)	Total Storage (AF)	Change in Reservoir (AF)	Releases (cfs)	Diversions (cfs)	Inflow (cfs)
01-Mar-15	7,809.00	25	0	7	0	7
02-Mar-15	7,808.96	25	0	7	0	7
03-Mar-15	7,808.88	24	-1	7	0	6
04-Mar-15	7,808.68	23	-1	7	0	6
05-Mar-15	7,808.36	22	-1	7	0	6
06-Mar-15	7,808.51	23	1	6	0	7
07-Mar-15	7,808.86	24	1	6	0	7
08-Mar-15	7,809.22	26	2	6	0	7
09-Mar-15	7,809.54	28	2	6	0	7
10-Mar-15	7,809.83	29	1	7	0	8
11-Mar-15	7,810.11	31	2	7	0	8
12-Mar-15	7,810.17	31	0	8	0	8
13-Mar-15	7,809.74	29	-2	8	0	7
14-Mar-15	7,809.67	29	0	8	0	8
15-Mar-15	7,809.97	30	1	8	0	9
16-Mar-15	7,810.55	34	4	8	0	10
17-Mar-15	7,811.02	37	3	9	0	11
18-Mar-15	7,811.01	37	0	11	0	11
19-Mar-15	7,810.84	35	-2	12	0	11
20-Mar-15	7,810.53	34	-1	13	0	12
21-Mar-15	7,810.41	33	-1	13	0	12
22-Mar-15	7,810.55	34	1	13	0	14
23-Mar-15	7,810.64	34	0	10	2	12
24-Mar-15	7,810.02	31	-3	7	5	10
25-Mar-15	7,809.55	28	-3	7	3	8
26-Mar-15	7,808.88	24	-4	6	4	8
27-Mar-15	7,808.95	25	1	6	1	8
28-Mar-15	7,810.12	31	6	7	3	13
29-Mar-15	7,810.48	33	2	7	13	21
30-Mar-15	7,810.37	33	0	7	14	21
31-Mar-15	7,810.61	34	1	8	16	25

	Releases (cfs)	Diversions (cfs)	Inflow (cfs)
AVERAGE IN CFS	8	2	10
TOTALS IN ACRE FEET	494	121	625

APPENDIX B

SUPPLEMENTAL DATA FOR THE EVALUATION OF ADDITIONAL NONVOLATILE TRACERS

This Appendix contains additional nonvolatile data that was evaluated for determining groundwater MTT. Figure 11 contains plots showing the relationship between West Fork spring ages and individual ion concentrations. Figure 12 shows the relationship between spring ages and specific conductivity (SC).

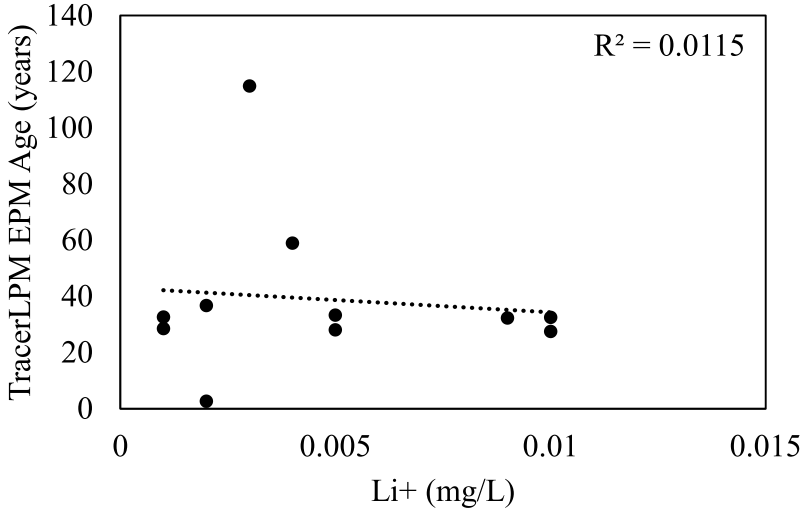

Figure 11. The relationship between West Fork spring ages and ion chemistry. The ages used in this analysis are from TracerLPM EPM results, and are presented in Table 2 in the main text. Ion concentrations are provided in Table 5, Appendix A. Note: the x-axis on the following charts is not uniform; each one is scaled according to the range of concentrations it represents. There is no plot for ammonium (NH_4^+) since this cation was not detected in any of the West Fork spring samples. Most of the ions investigated show no apparent correlation to West Fork spring ages. Although the most elevated chloride (Cl^-) concentrations do relate nicely to the oldest ages, chloride concentrations for younger water are not uniquely related to age. Therefore, it is unlikely that Cl^- would be widely applicable for determining groundwater MTT since many watersheds, like the West Fork, likely contain a significant fraction of water < 50 years old. Also note, the relationship between age and NO_2^- is based on only four springs at which NO_2^- was measureable, and is therefore considered unreliable.

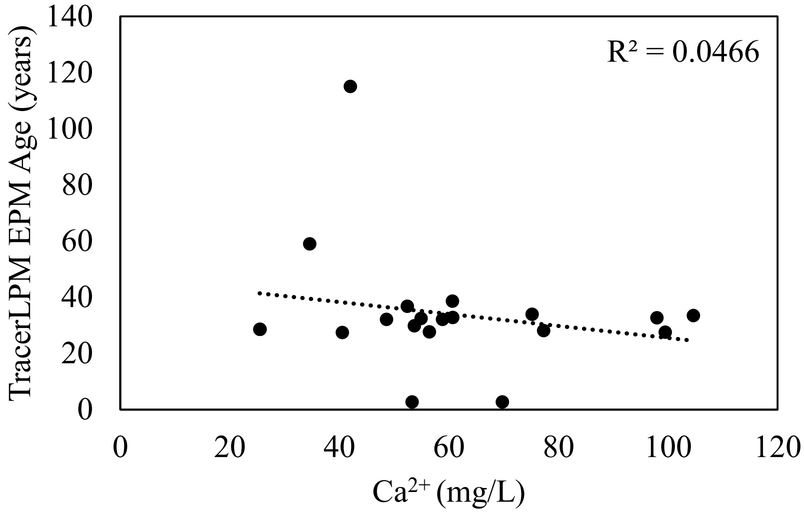

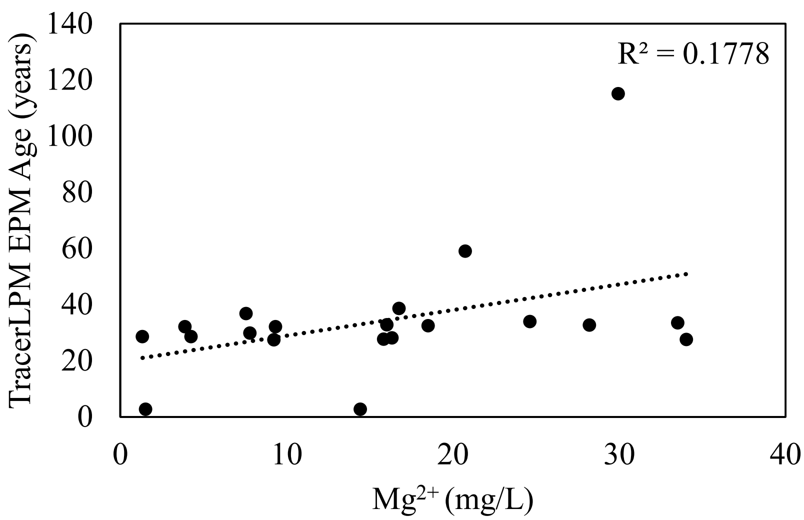

Figure 11. continued

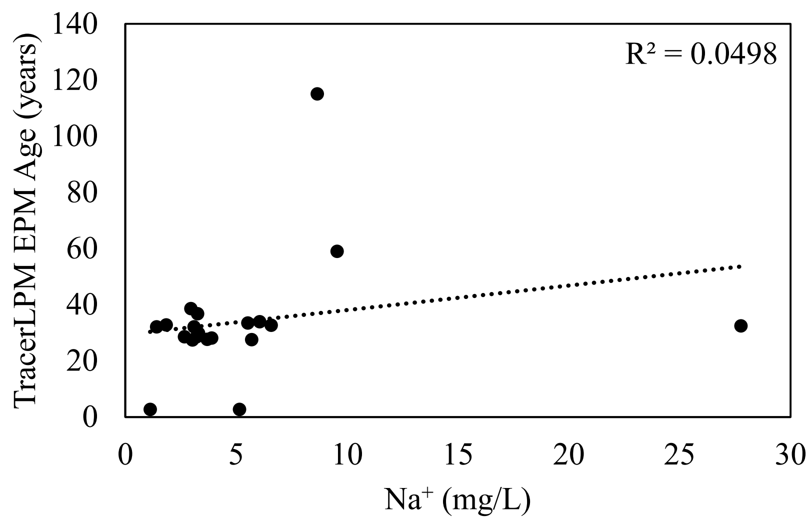

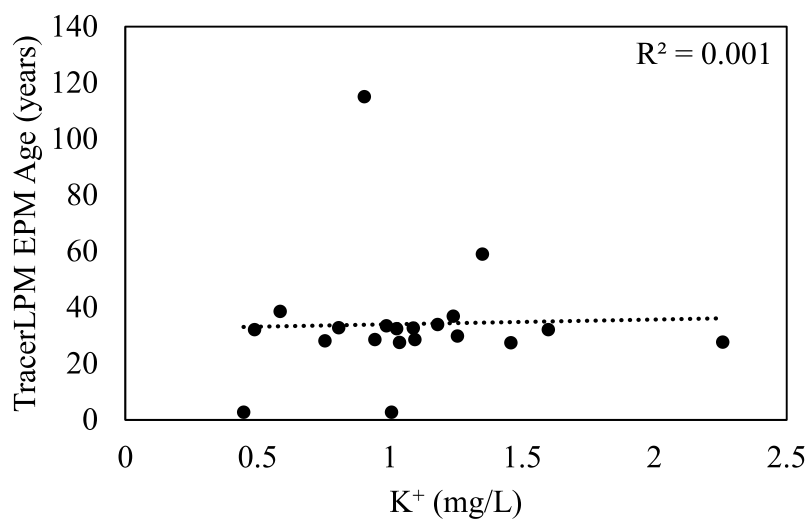

Figure 11. continued

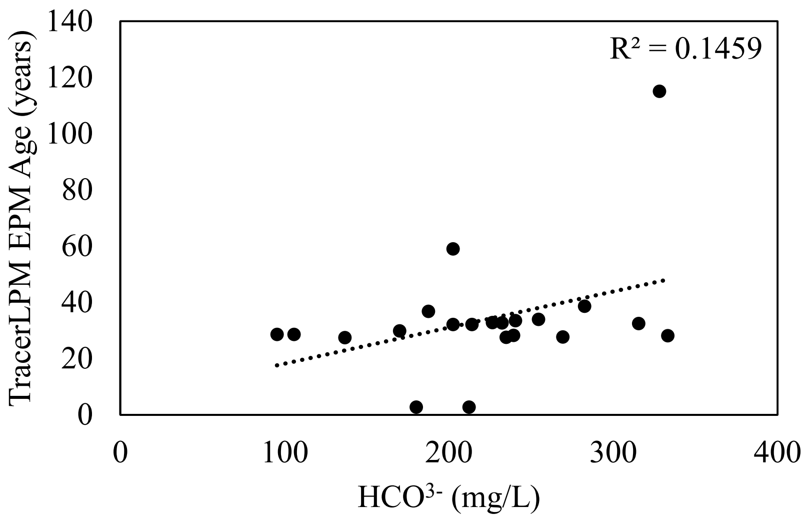

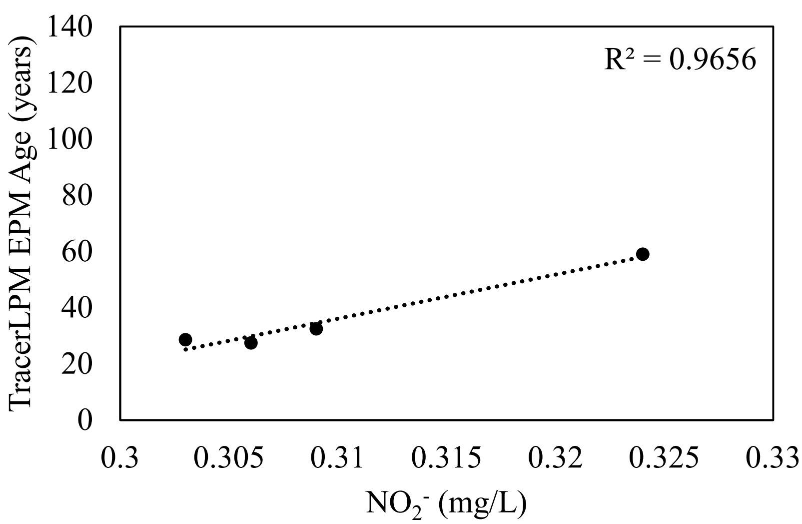

Figure 11. continued

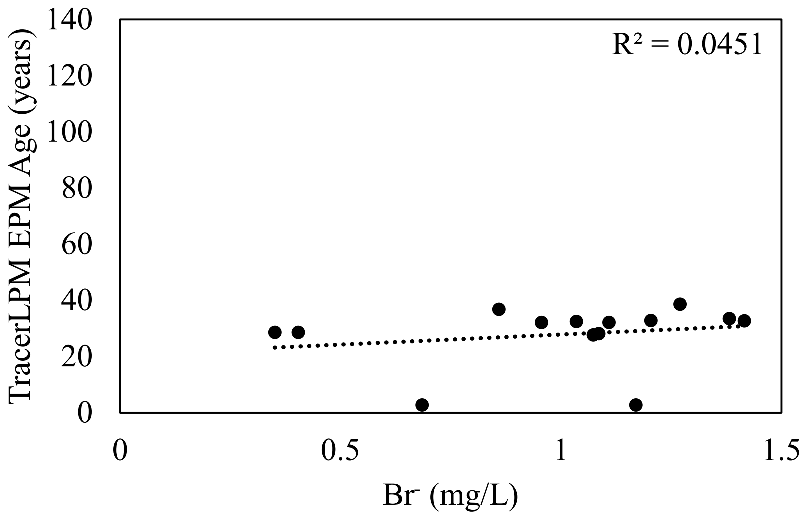

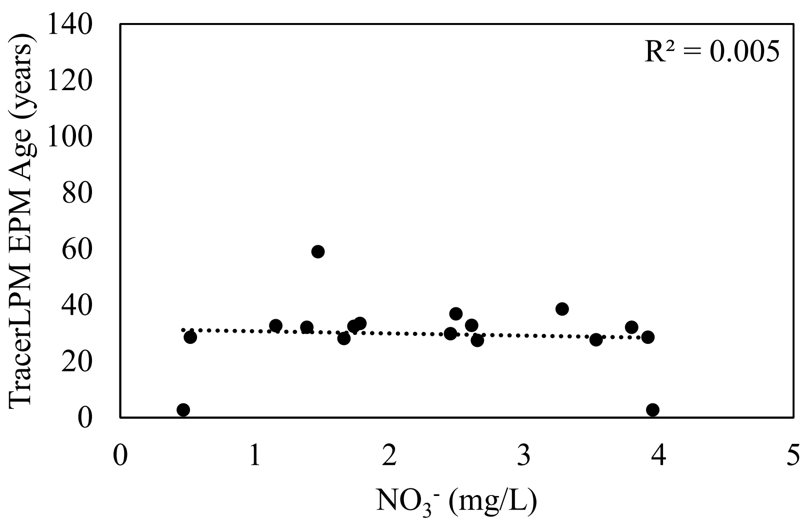

Figure 11. continued

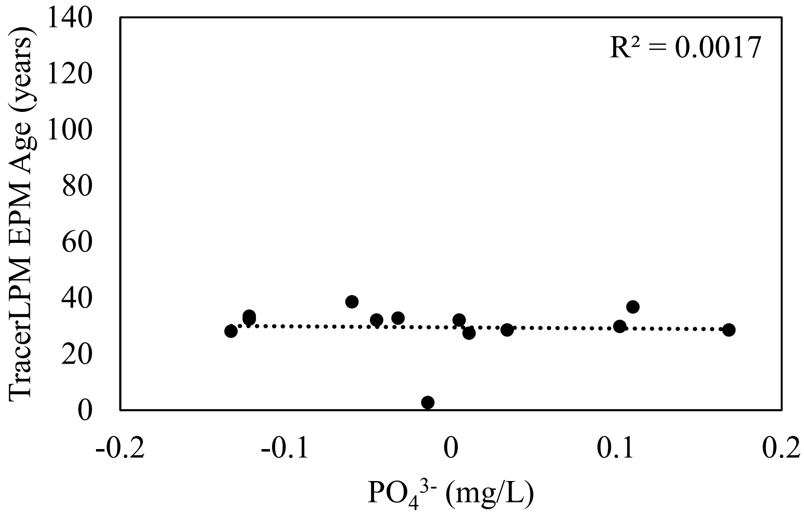

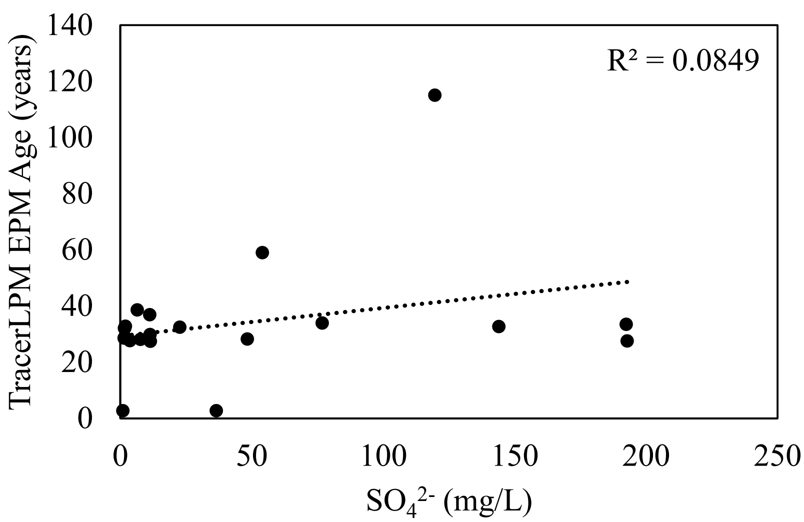

Figure 11. continued

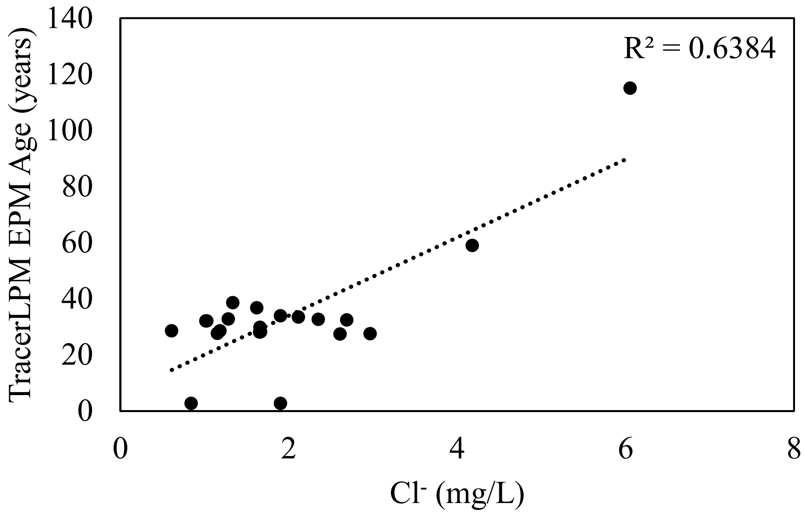

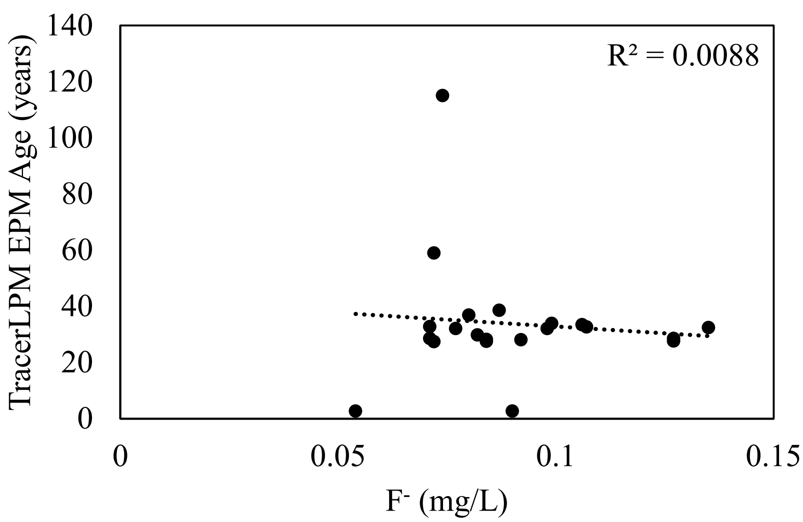

Figure 11. continued

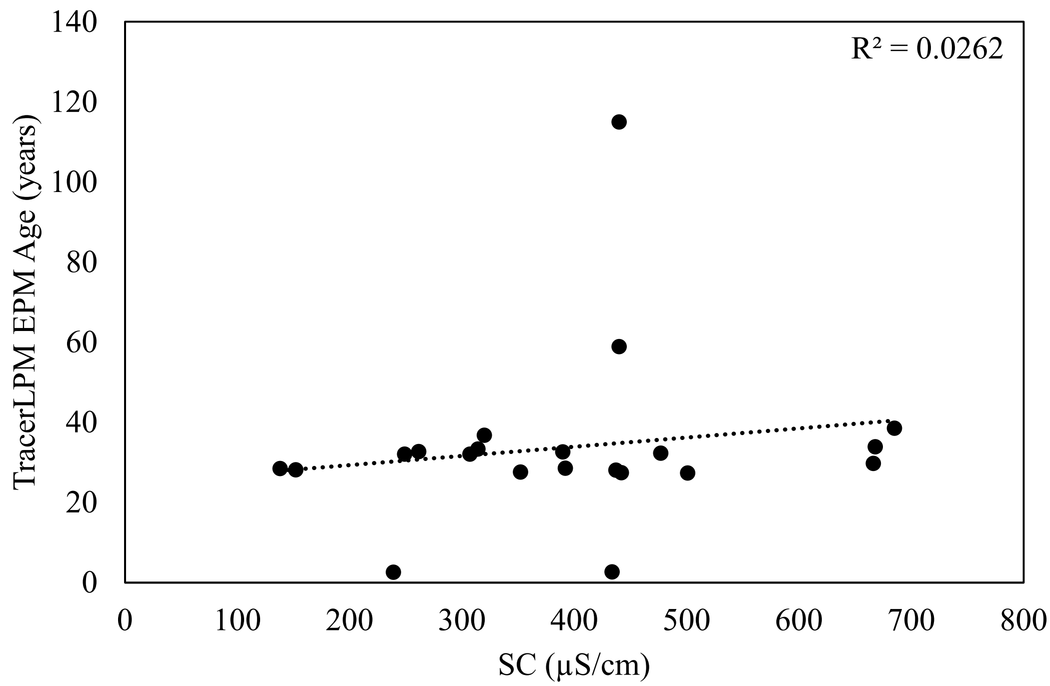

Figure 12. The relationship between West Fork spring ages and specific conductivity. SC was measured with a Hydrolab Multiprobe during each sampling visit; values are presented in Table 4, Appendix A. There is no apparent correlation between West Fork spring ages determined from lumped-parameter modeling of environmental tracer concentrations and West Fork spring SC.

REFERENCES

Aeschbach-Hertig, W., and D.K. Solomon, 2013, Noble gas thermometry in groundwater hydrology, in P. Burnard, ed., The noble gases as geochemical tracers: Berlin Heidelberg, Springer, p. 81-122.

Ashland, F.X., C.E. Bishop, M. Lowe, and B.H. Mayes, 2001, The geology of the Synderville Basin, Western Summit County, Utah, and its relation to groundwater conditions, Utah Geological Survey Open-File Report 337: Utah Department of Natural Resources Water Resources, Salt Lake City, 59 p.

Busenberg, E., and L.N. Plummer, 1992, Use of chlorofluorocarbons (CCl_3F and CCl_2F_2) as hydrologic tracers and age-dating tools: The alluvium and terrace system of central Oklahoma: Water Resources Research., v. 28, p. 2257–2283.

Bryant, B., 2010, Geologic map of the east half of the Salt Lake City 1° x 2° quadrangle (Duchesne and Kings Peak 30' x 60' quadrangles), Duchesne, Summit, and Wasatch Counties, Utah, and Uinta County, Wyoming: U.S. Geological Survey Miscellaneous Investigation Series Map I-1997, 1992, Miscellaneous Publication 10-1DM, scale 1:125,000, 3 sheets.

Central Utah Water Conservancy District (CUWCD), 2015, Vat diversion dam operation, central Utah project, diversion records March 2013- March 2014.

Constenius, K.N., D.L. Clark, J.K. King, and J.B. Ehler, 2011, Interim geologic map of the Provo 30’ x 60’ quadrangle, Utah, Wasatch and Salt Lake Counties, Utah: Utah Geological Survey Open-File Report 586DM, scale 1:62,500.

Cook, P.G., and J.K. Böhlke, 2000, Determining timescales for groundwater flow and solute transport, in P.G. Cook, and A.L. Herczeg, ed., Environmental tracers in subsurface hydrology: Norwell, Kluwer Academic Publishers, p. 1-30.

Cook, P.G., G. Favreau, J.C. Dighton, and S. Tickell, 2003, Determining natural groundwater influx to a tropical river using radon, chlorofluorocarbons and ionic environmental tracers: Journal of Hydrology, v. 227, p. 74-88, doi 10.1016/S0022-1694(03)00087-8.

Cook, P. G., and D.K. Solomon, 1995, Transport of atmospheric trace gases to the water table: Implications for groundwater dating with chlorofluorocarbons and krypton 85: Water Resources Research, v. 31, p. 263–270.

Cook, P.G., and D.K. Solomon, 1997, Recent advances in dating young groundwater: chlorofluorocarbons, $^{3}H/^{3}He$ and ^{85}Kr: Journal of Hydrology, v. 191, p. 245–265, doi 10.1016/S0022-1694(96)03051-X.

The University of Utah, 2015, Dissolved and noble gas lab, http://www.noblegaslab.utah.edu/index.html (accessed November 2015).

Eastoe, C.J., C.J. Watts, M. Ploughe, and W.E. Wright, 2012, Future use of tritium in mapping pre-bomb groundwater volumes: Ground Water, v. 50, p. 87–93, doi 10.1111/j.1745-6584.2011.00806.x.

Freethey, G.W., and G.E. Cordy, 1991, Geohydrology of the Mesozoic rocks in the Upper Colorado River Basin in Arizona, Colorado, New Mexico, Utah, and Wyoming: USGS Professional Paper 1411-C, 130 p.

Freeze, R.A., and J.A. Cherry, 1979, Groundwater: Englewood Cliffs, Prentice-Hall, p. 604.

Frisbee, M.D., F.M. Phillips, A.R. Campbell, F. Liu, and S.A. Sanchez, 2011, Streamflow generation in a large, alpine watershed in the southern Rocky Mountains of Colorado: Is streamflow generation simply the aggregation of hillslope runoff responses?: Water Resources Research, v. 47, p. 1–18, doi 10.1029/2010WR009391.

Gee, K., 1994, Flagstaff Mountain at Deer Valley - an expansion of the Deer Valley Resort and the hydrogeology of the Judge Tunnel, Park City, Utah: Park City, Utah unpublished consultant's report, p. 6.

Genereux, D.P., and H.F. Hemond, 1990, Naturally occurring radon 222 as a tracer for streamflow generation: steady state methodology and field example: Water Resources Research, v. 26, iss. 12, p. 3065-3075, doi 10.1029/WR026i012p03065.

Jurgens, B.C., J.K. Böhlke, and S.M. Eberts, 2012, TracerLPM (Version 1): An Excel® workbook for interpreting groundwater age distributions from environmental tracer data: U.S. Geological Survey Techniques and Methods Report 4-F3, 60 p.

Koh, D.C., L.N. Plummer, E. Busenberg, and Y. Kim, 2007, Evidence for terrigenic SF_6 in groundwater from basaltic aquifers, Jeju Island, Korea: Implications for groundwater dating: Journal of Hydrology, v. 339, p. 93–104.

Kralik, M., F. Humer, J. Fank, T. Harum, G. Klammler, D. Gooddy, J. Sültenfuß, C. Gerber, and R. Purtschert, 2014, Using $^{18}O/^{2}H$, $^{3}H/^{3}He$, ^{85}Kr and CFCs to determine mean residence times and water origin in the Grazer and Leibnitzer Feld groundwater bodies (Austria): Applied Geochemistry, v. 50, p. 150–163.

McMahon, P.B., L.N. Plummer, J.K. Bölke, S.D. Shapiro, and S.R. Hinkle, 2011, A comparison of recharge rates in aquifers of the United States based on groundwater-age data: Hydrogeology Journal, v. 19 no. 4, p. 779 – 800, doi 10.1007/s10040-0110722-5.

Miller, M.P., D.D. Susong, C.L Shope, V.M. Heilweil, and B.J. Stolp, 2014, Continuous estimation of baseflow in snowmelt-dominated streams and rivers in the Upper Colorado River Basin: A chemical hydrograph separation approach: Water Resources Research, v. 50, p. 6986–6999, doi 10.1002/2013WR014939.

Morgenstern, U., M.K. Stewart, and R. Stenger, 2010, Dating of streamwater using tritium in a post nuclear bomb pulse world: Continuous variation of mean transit time with streamflow: Hydrology and Earth System Science, v. 14, p. 2289–2301, doi 10.5194/hess-14-2289-2010.

Peters, N.E., D.A. Burns, and B.T. Aulenbach, 2014, Evaluation of high-frequency mean streamwater transit-time estimates using groundwater age and dissolved silica concentrations in a small forested watershed: Aquat. Geochemistry, v. 20, p. 183–202 doi 10.1007/s10498-013-9207-6.

Plummer, L.N., E. Busenberg, and L.F. Han, 2006, CFCs in binary mixtures of young and old groundwater, use of chlorofluorocarbons in hydrology: A guidebook, International Atomic Energy Agency (IAEA), v .5, chapt. 5, p. 59-72.

PRISM Climate Group, 2014, Average annual precipitation (1981-2010): Utah, http://prism.oregonstate.edu (accessed November 2015).

PRISM Climate Group, 2015, Average annual mean temperature: 2014, http://prism.oregonstate.edu (accessed November 2015).

Robson, S.G., and E.R. Banta, 1995, Ground water atlas of the United States: segment 2, Arizona, Colorado, New Mexico, Utah: Hydrologic atlas 730-C U.S. Geological Survey, C1-C32.

Rueedi, J., M.S. Brennwald, R. Purtschert, U. Beyerle, M. Hofer, R. Kipfer, J.V. Turner, and P.K. Aggarwal, 2005, Estimating amount and spatial distribution of groundwater recharge in the Iullemmeden basin (Niger) based on ^{3}H, ^{3}He and CFC-11 measurements: Hydrological Processes, v. 19, p. 3285–3298.

Schlosser, P., M. Stute, H. Dörr, C. Sonntag, and K.O. Münnich, 1988, Tritium/^{3}He dating of shallow groundwater: Earth and Planetary Science Letters, v. 89, p. 353–362.

Schwientek, M., P. Maloszewski, and F. Einsiedl, 2009, Effect of the unsaturated zone thickness on the distribution of water mean transit times in a porous aquifer: Journal of Hydrology, v. 373, p. 516–526.

Solomon, D.K., and P.G. Cook, 2000, ^{3}H and ^{3}He, in P.G. Cook, and A.L. Herczeg, ed., Environmental tracers in subsurface hydrology, Norwell, Kluwer Academic Publishers, p. 397-424, doi 10.1007/978-1-4615-4557-6_13.

Solomon, D.K., S.L. Schiff, R.J. Poreda, and W.B. Clarke, 1993, A validation of the ^{3}H/^{3}He method for determining groundwater recharge: Water Resources Research, v. 29, p. 2951–2962, doi 10.1029/93WR00968.

Stewart, M.K., J. Mehlhorn, and S. Elliott, 2007, Hydrometric and natural tracer (oxygen-18, silica, tritium and sulphur hexafluoride) evidence for a dominant groundwater contribution to Pukemanga Stream, New Zealand: Hydrological Processes, v. 21, p. 3340-3356, doi 10.1002/hyp.6557.

Uygur,K., and M.D. Picard, 1984, Implications to exploration of porosity relationships and paragenitic sequences, Jurassic Navajo (Nugget) Sandstone, Utah and Southwestern Wyoming: AAPG Bulletin, v. 01/1984: p. 68, doi 10.1306/AD461656.

USGS, 2015, Reston groundwater dating laboratory, http://water.usgs.gov/lab (accessed November 2015).

Utah AGRC, 2016, Base map and imagery, http://gis.utah.gov (accessed November 2015).

Wilkowske, C.D., D.V. Allen, and J.V. Phillips, 2003, Drought conditions in Utah during 1999-2002: a historical perspective, USGS fact sheet 037-03: United States Geological Survey Reston, VA, 6 p.

Zoellmann, K., W. Kinzelbach, and C. Fulda, 2001, Environmental tracer transport (^{3}H and SF_6) in the saturated and unsaturated zones and its use in nitrate pollution management: Journal of Hydrology, v. 240, p. 187–205.